FACTA UNIVERSITATIS
Series: **Electronics and Energetics** Vol. 28, N° 3, September 2015, pp. 345 - 381
DOI: 10.2298/FUEE1503345J

RF MEMS/NEMS RESONATORS FOR WIRELESS COMMUNICATION SYSTEMS AND ADSORPTION-DESORPTION PHASE NOISE

Ivana Jokić[1,2], Miloš Frantlović[1,2], Zoran Djurić[3], Miroslav L. Dukić[4]

[1]School of Electrical Engineering, University of Belgrade, Bulevar Kralja Aleksandra 83, 11000 Belgrade, Serbia
[2]Institute of Chemistry, Technology and Metallurgy - Center of Microelectronic Technologies, University of Belgrade, Njegoševa 12, 11000 Belgrade, Serbia
[3]Serbian Academy of Sciences and Arts, Institute of Technical Sciences SASA, Knez Mihailova 35, 11000 Belgrade, Serbia
[4]Singidunum University, Danijelova 29, 11000 Belgrade, Serbia

Abstract. *During the past two decades a considerable effort has been made to develop radio-frequency (RF) resonators which are fabricated using the micro/nanoelectro-mechanical systems (MEMS/NEMS) technologies, in order to replace conventional large off-chip components in wireless transceivers and other high-speed electronic systems.*
The first part of the paper presents an overview of RF MEMS and NEMS resonators, including those based on two-dimensional crystals (e.g. graphene). The frequency tuning in MEMS/NEMS resonators is then analyzed. Improvements that would be necessary in order for MEMS/NEMS resonators to meet the requirements of wireless systems are also discussed.
The analysis of noise of RF MEMS/NEMS resonators and oscillators is especially important in modern wireless communication systems due to increasingly stringent requirements regarding the acceptable noise level in every next generation. The second part of the paper presents the analysis of adsorption-desorption (AD) noise in RF MEMS/NEMS resonators, which becomes pronounced with the decrease of components' dimensions, and is not sufficiently elaborated in the existing literature about such components. Finally, a theoretical model of phase noise in RF MEMS/NEMS oscillators will be presented, with a special emphasize on the influence of the resonator AD noise on the oscillator phase noise.

Key words: *MEMS resonator, NEMS resonator, tunable resonator, graphene resonator, adsorption-desorption noise, oscillator phase noise*

Received March 2, 2015
Corresponding author: Zoran Djurić
Serbian Academy of Sciences and Arts, Institute of Technical Sciences SASA,
Knez Mihailova 35, 11000 Belgrade, Serbia
(e-mail: zoran.djuric@itn.sanu.ac.rs)

1. INTRODUCTION

Over the past two decades, wireless communications have been a subject of intensive development, and tremendous growth has taken place in this area of technology and industry. Modern wireless terminals have become universal mobile personal devices which unite the functions of a telephone, a computer with Internet access, a radio navigational device, a multimedia center etc., and in every new generation operate in a greater number of frequency ranges (multiband operation) and according to a greater number of communication standards (multistandard operation). This course of development poses new challenges related to the design of these devices' transceivers. Having in mind the requirements for a small size, low power consumption and low cost of mobile terminals, it is apparent that the multiband multistandard front end, i.e. the transceiver part in which the processing of high frequency signals is performed, is the most critical.

In transceivers operating at frequencies around 1 GHz and higher, which is common in modern mobile personal devices, it is still not technologically possible to ensure entirely software-based adaptation to an arbitrary communication standard. The processing of signals at those frequencies (filtering, amplification, frequency conversion) is performed by analog circuits, and it often requires the implementation of off-chip (discrete) passive components and several separate integrated circuits (IC), because the performance of the corresponding integrated components and circuits implemented in CMOS technology are not satisfactory. Bearing in mind the trend towards an increasing number of frequency bands in which a mobile terminal is used, the current approach towards designing multiband multistandard transceivers, which implies the introduction of an additional set of RF analog circuits and off-chip passive components for each new band and wireless standard, is becoming inefficient because it leads to an unacceptable increase in complexity, power consumption, size and price. Particularly critical is the increase in the number of off-chip passive RF components. In the next generation of mobile terminals, the reconfigurability of the RF part of transceivers should be achieved by using as small a number of components as possible, with the simultaneous increase in the integration level: by replacing the discrete passive components (such as RF filters, duplexers, switches, impedance matching circuits, resonators in frequency references and frequency synthesizers, etc.) with integrated ones, by introducing components with tunable parameters instead of a number of discrete ones with fixed parameters; the most desirable solution implies the application of integrated tunable (reconfigurable) passive components. However, in this regard, the possibilities of conventional technologies are limited.

The requirements for the reconfigurability of the RF front-end, better RF performance and a higher level of integration of the RF segment of the transceiver in future systems generate the need for high-quality passive RF components, applicable in a wide frequency range, as well as for those with tunable parameters, which will be integrated in CMOS circuits. Nowadays, MEMS and NEMS technologies are considered to have the potential for the realization of RF components which are able to meet the mentioned requirements.

RF MEMS/NEMS resonators are being developed with the intention to replace large off-chip components, such as RF filters and quartz resonators, in wireless transceivers [1-4]. In the first part of this paper we present a short overview of RF MEMS resonators, including their classifications, principle of operation, their main characteristics relevant for wireless transceiver applications and advantages compared to solutions based on

conventional technologies. The achieved values of basic parameters will be given through examples of RF MEMS resonators reported in the literature. The capability of RF MEMS and NEMS resonators to meet future needs will also be considered, including the possibility of frequency tuning in MEMS and NEMS mechanical resonators. Resonators based on two-dimensional (2D) crystals (such as graphene) will also be included in the analysis. The comment will be given on the necessary improvements and the direction of future research in this field, with the intention to optimize RF MEMS and NEMS components according to requirements of both current and future systems, especially having in mind the need for NEMS resonators. The analysis of noise generation mechanisms which are specific for these components is of particular significance in this respect: it leads to optimal resonator's design and operating conditions, which ensure minimal noise and, accordingly, minimization of signal degradation. In the second part of the paper we will present the analysis of adsorption-desorption (AD) noise in RF MEMS and NEMS electromechanical resonators, which becomes pronounced with components' decreasing dimensions and mass. Finally, we present a theoretical model of phase noise in oscillators using RF MEMS/NEMS resonators as frequency determining elements, considering the influence of the resonator AD noise.

2. RF MEMS AND NEMS RESONATORS

Radio-frequency MEMS and NEMS technologies are intended for the realization of MEMS and NEMS passive components - variable capacitors, inductors, resonators, switches, which may be basic elements of more complex functional blocks such as tunable filters, impedance-matching networks, phase shifters, reference oscillators, frequency synthesizers, antenna switches etc, all of them operating at radio frequencies to mm-wave frequencies (i.e. up to the order of 10 GHz and above). The development of RF MEMS components began at the end of 1980s. High RF performance (even of tunable components), dimensions at the micrometer scale, the technological compatibility with CMOS and other IC technologies which enable their integration with active electronics, low power consumption, and mass production, make them promising candidates for application in wireless transceivers. Integrated RF MEMS components can directly replace off-chip traditional components (RF filters and crystal oscillator references, as well as other passives and RF switches) in conventional transceiver architectures, as shown in Fig. 1a. Furthermore, tunable RF MEMS components can be used to ensure front-end reconfigurability in multiband multistandard transceivers, significantly reducing its complexity, as shown in Fig. 1b.

2.1. RF MEMS resonators – A short overview of existing components and future needs

Resonator is a basic element of oscillators and frequency selective circuits. The applications of resonators in wireless transceivers are numerous. They include RF filters and duplexers, tunable tanks of voltage controlled oscillators (VCOs), frequency references, frequency synthesizers, clock generators. The basic parameters of resonators are the resonance frequency, f_0, and the quality factor, Q, while other important parameters are frequency stability (in time – e.g. long/short-term; with temperature; with pressure etc.), power handling capability and series resistance. The value of the product $f_0 \cdot Q$ is often

used as an indicator of the performance of the resonator. The required values of the resonator parameters depend on its application. For example, resonance frequencies of resonators used in various stable frequency references (for the operation of cellular modules, GPS modules, microprocessors, real-time clocks etc.) and filters with different central frequencies in wireless transceivers cover a wide range (f_0 are of the order of 1 kHz – 1 GHz). The quality factor of a VCOs resonant tank in a superheterodyne receiver can be 30–50, but Q of RF bandpass filters, with the central frequencies in the range 0.8–5.5 GHz, must be much greater (Q~500–10000). The highest Q (typically greater than 10^5, even 10^6) is required in frequency references (oscillators). The temperature frequency stability of frequency references in mobile terminals should be better than ±10 ppm in the range 0–70 ºC [2]. The maximal acceptable resonator frequency variation for frequency synthesis is ±2 ppm in the same temperature range. In RF preselect filters and image-rejection filters the maximum temperature coefficient of frequency can be ~10 ppm/ºC. The resonator long-term frequency stability better than 3 ppm/year is needed [4]. The resistance should be low enough to allow impedance matching to conventional RF circuits (typically 50 Ω).

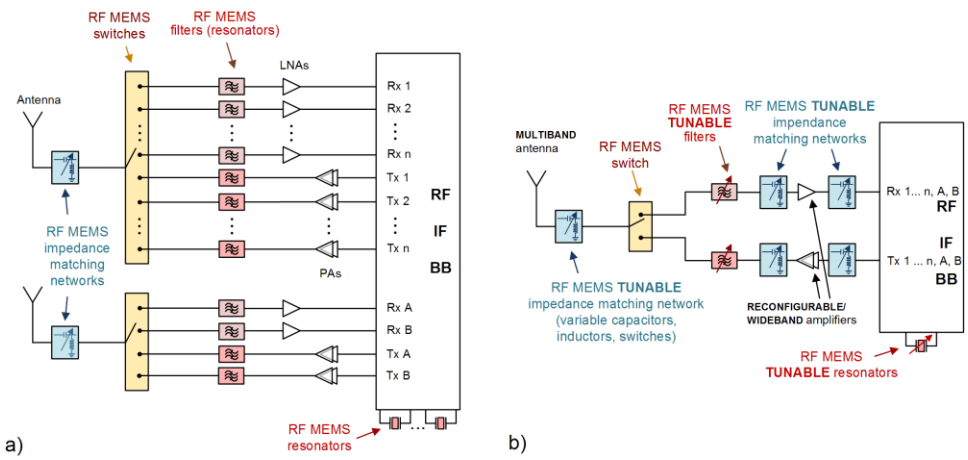

Fig. 1 Simplified block-diagram of a hypothetical multiband multistandard wireless transceiver RF front end, illustrating applications of RF MEMS components (shown in color/gray): a) direct replacement of non-integrated conventional components with integrated MEMS components, b) significantly simplified RF front end as a result of the application of tunable MEMS components.

Resonators can generally be divided into electromagnetic and electromechanical. In modern wireless transceivers, electromagnetic resonators are LC circuits, while electromechanical ones include SAW (Surface Acoustic Wave) and BAW (Bulk Acoustic Wave) resonators. SAW and BAW resonators (which also include quartz resonators) are off-chip components, and have better performance than electromagnetic ones, especially than integrated ones. SAW resonators are used in high-performance RF filters and duplexers, with central frequencies up to 2 GHz. The nominal frequencies of crystal resonators are of the order of 10 kHz–10 MHz. With the increase in the resonance frequency

of quartz resonators, the value of the Q factor decreases. The best quartz resonators (whose production is complex and expensive) with a frequency of 10 MHz have $Q=10^6$. The series resistance of quartz resonators is 50 Ω, whereas the frequency stability, at best 1 ppm, in the temperature range of 100°C may be achieved by choosing the optimum oscillating mode and crystal cut. Conventional resonators are highly reliable and technologically mature, but none of the mentioned resonator types can simultaneously meet the following requirements: resonance frequencies in GHz-range, high Q at GHz-frequencies, tunability, low power consumption, high frequency stability, small dimensions, low cost and integration (especially monolithic) with CMOS circuits. Therefore, they are an obstacle for full integration and miniaturization of GHz multiband multistandard wireless transceivers.

During the past two decades a considerable effort has been made in the development of RF MEMS resonators in order for them to be used in wireless transceivers instead of conventional bulky off-chip resonators [1-4]. Both electromagnetic and electromechanical resonators have been fabricated using the MEMS technology. As far as MEMS resonators of these two types with equal resonance frequency are concerned, MEMS electromechanical resonators are smaller and have a higher quality factor than electromagnetic ones. In the following text we will present electromechanical (EM) RF MEMS resonators in greater detail.

Some of the main advantages that MEMS technologies bring into the field of EM resonators include small dimensions, high both f_0 and $f_0 \cdot Q$ product (f_0 up to the order of 1 GHz, Q comparable to conventional), low power consumption, the possibility of low-cost mass production and integration (monolithic or hybrid) with CMOS ICs. An especially attractive feature of MEMS resonators is the tunability of their parameters.

EM resonators consist of the resonant mechanical structure and the input and output electromechanical transducer. The operation of EM resonators is based on mechanical oscillations of a resonant structure, which are actuated by the input electrical signal and converted in the output electrical signal. An input EM transducer converts electrical energy into mechanical energy (i.e. electric voltage into force or mechanical stress), whereas an output transducer converts mechanical energy into electrical energy (i.e. displacement or deformation of the resonant structure into an output electrical signal). The actuation is usually achieved through the action of electrostatic (ES) or magnetic force, or it is based on a piezoelectric (PE) effect or on thermally induced expansion. The mechanism of conversion of mechanical energy into an electrical signal can be capacitive, piezoelectric, piezoresistive, etc. The most common are the combination of ES (capacitive) actuation and capacitive detection of mechanical oscillations and the combination of PE actuation and detection.

Electromechanical transducers are characterized by the coefficient of electromechanical coupling, which is a measure of the efficiency of energy conversion between electrical and mechanical domains of a resonator. It depends on the shape and dimensions of the resonant structure, material parameters, mode of oscillation, the transduction mechanism, the transducer's parameters, as well as the position and size of electrodes, and it significantly influences the parameters of the resonator (e.g. the equivalent series resistance) [3].

The capacitive actuation and detection of mechanical oscillation of the resonant structure are achieved as shown in Fig. 2a. DC voltage V_P is applied to the resonant structure, whereas alternating driving voltage v_i is applied to the input electrode. These

two voltages together generate time-variable electric force acting on the resonant structure and exciting its mechanical resonant oscillation if the frequency of the excitation electrical signal is equal to the mechanical resonance frequency of the structure (which depends on the geometrical parameters of the resonant structure and parameters of the materials from which it is made). During the resonant oscillation of the structure, the distance between the structure and the output electrode changes in time. Consequently, the corresponding capacitance and the output current also change, this change being directly proportional to the instantaneous value of the oscillation amplitude and bias voltage V_p. Accordingly, the output current is generated only if $V_p \neq 0$, and the capacitive resonators are switched on and off by a simple mechanism (by turning the polarization voltage on and off). In order to achieve low power consumption and integrability with the integrated circuits, the value of V_p should be low enough. Therefore, the distance g between the electrodes of capacitive transducers and the resonant structure should be less than 1 μm. A smaller electrode gap and a greater surface area of electrodes ensure a greater EM coupling coefficient. The coupling coefficient in ES transduction depends on the bias voltage (it is directly proportional).

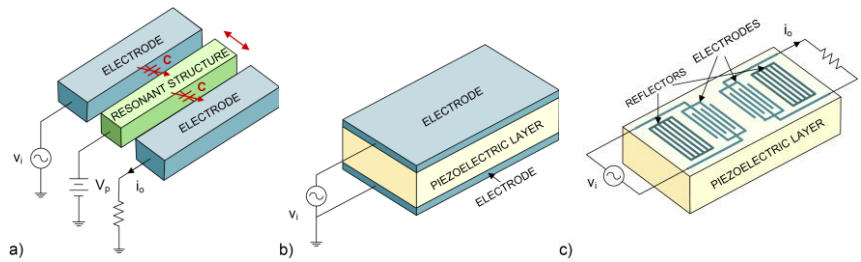

Fig. 2 Schematic representation of MEMS resonators, illustrating their basic electro-mechanical configuration and principle of operation: a) a resonator with capacitive actuation and detection of mechanical oscillation, b) with piezoelectric (PE) actuation and detection of bulk acoustic waves, c) with PE actuation and detection of surface acoustic waves.

The resonant structure of capacitive resonators can be in the shape of a cantilever, clamped-clamped or free-free beam, membrane, disk, quadratic plate, ring or comb. They are usually made of silicon, but silicon carbide, silicon nitride, diamond, germanium, silicon germanium, gallium arsenide, nickel, etc. can also be used. The most common configurations of electrodes are parallel plates, and interdigitated (comb) electrodes. A conducting material or a dielectric covered with a thin conductive layer can be used to manufacture electrodes. Electrodes are placed in such a way to maximize coupling into a desired mode of vibration. Capacitive resonators oscillate in flexural or torsional modes, but there are also capacitive resonators with bulk oscillation modes: extensional longitudinal, extensional contour (i.e. radial for disk resonators), wine-glass and Lamé.

The piezoelectric mechanism of excitation and detection of mechanical waves is based on the use of piezoelectric materials which are prone to mechanical deformation in the presence of an electric field (inverse PE effect), while the induced mechanical deformation of the material generates a voltage at the output port (PE effect). The main functional

components of the resonator are a layer of a PE material (e.g. AlN, ZnO, lead zirconate titanate (PZT)), reflector structures (surfaces) and the electrodes to which the driving electric signal is applied, or which are used to detect the generated voltage (Figs. 2b and 2c). Metal electrodes are placed directly on the PE layer. PE layer is usually in the form of a square, rectangular or circular plate but they may also have a form of a circular or square ring. Driving electrical signal excites acoustic waves in PE material, and the reflector surfaces confine the generated acoustic waves. This enables the acoustic resonance to be established, when the frequency of the excitation electrical signal is equal to the mechanical resonance frequency determined by the geometry of the system and the parameters of the material. There are several types of PE RF MEMS resonators, but they can generally be divided into SAW and BAW resonators. In a SAW resonator, input and output interdigitated electrodes and reflectors are placed on the same surface of the PE layer. In BAW resonators, a thin layer of a PE material is placed between the electrodes. In SAW and BAW resonators, mechanical waves are formed on the surface and within the volume of the thin layer of a PE material, respectively. SAW resonators usually oscillate in the Rayleigh mode. The most common oscillating modes in BAW resonators are the bulk extensional mode in the direction of piezolayer thickness, i.e. the direction of the excitation electrical field (such as in FBARs – thin Film Bulk Acoustic Resonators), or the lateral extensional mode (in LBARs – Lateral BARs). The resonance frequency of FBAR depends on the thickness of the PE layer. The FBAR resonance in the range of lower GHz frequencies is formed in the layers of the PE material reaching about 1 μm in thickness, whereas the lateral dimension of the resonator are of the order of 10-100 μm. The lateral extension modes may be along one direction or a contour, whereas the resonance frequency is determined by the lateral dimensions (e.g. the width of the ring acting as the resonant structure). The lateral bulk modes can also be formed in hybrid SAW-BAW structures, in which the direction of the excitation electric field belongs to the lateral plane (LFER – Lateral Field-Excited Resonator). The interdigitated electrodes of these resonators are located on a single surface of the PE layer (just like in a SAW resonator), bulk standing acoustic waves are formed (as in BAW resonators), whereas the resonance frequency is determined by the distance between two adjacent "fingers" of interdigital electrodes (the lateral dimension, as in SAW resonators). Less commonly, PE actuation is used to excite the flexural modes of oscillation of suspended resonant structures comprising a layer(s) of PE material [5].

In the piezoelectric mechanism of energy conversion, the coefficient of EM coupling is larger than in the capacitive mechanism, for resonators of similar shape and size. It is greater in FBAR resonators than in LBARs. AlN resonators have a slightly smaller coupling coefficient than ZnO and PZT components, but their piezoelectric properties are excellent and they are suitable for high-frequency applications [6].

The mechanical resonant frequency of the structure is determined by its stiffness and mass, i.e. by its geometry, dimensions and material parameters. The Q factor of the resonator (unloaded Q) is by definition equal to the ratio of the energy stored in the resonator and the energy lost per one cycle of oscillation. A high resonator Q results in low resonator impedance (i.e. series resistance). The fulfillment of requirements to be met by an oscillator in terms of phase noise and frequency stability, as well as the filter insertion loss and selectivity, power dissipation, etc. also depend on the Q value. The value of Q is determined by different mechanisms of energy loss, both internal and

external. External loss mechanisms may include the loss of mechanical energy in places where the resonant structure is fixed during oscillation, or they can be a result of the presence of the surrounding medium (e.g. air or other gas mixtures) or external circuits. As for internal mechanisms, mechanical energy is dissipated in the resonator or on the surface of the resonant structure as a result of the presence of the bulk and surface defects, and thermoelastic effects that lead to the irreversible transformation of acoustic energy into heat [3]. With the increase of gas pressure in the surrounding medium inside the resonator cavity, the energy loss due to the gas damping can grow and prevail over losses caused by other mechanisms. Therefore, it is usually necessary to ensure that resonators operate in a vacuum packaging. The value of the pressure at which Q begins to decrease due to gas damping with further increase in pressure depends on the resonance frequency and dimensions of the resonant structure. This pressure value is lower in resonators of smaller dimensions (at the same f_0), as well as in resonators of lower f_0. The energy loss due to other mechanisms can be minimized by optimizing the design of the resonator (choice of material, shape, size and place where the resonant structure is fixed, choice of mode of oscillation, etc.). For example, Q increases with a decreased resonator surface-to-volume ratio. Bulk mode resonators have a greater Q than flexural, whereas Si bulk resonators have greater Q than AlN bulk resonators. Thermoelastic losses set the upper fundamental thermodynamic limit of the resonator quality factor, and also of the $f_0 \cdot Q$ product in resonators whose resonant frequency is lower than 1 GHz [7]. The value of Q increases with decreasing temperature.

The resonance frequency of FBAR resonators is typically in the range between 400 MHz and 10 GHz, and their Q factor is usually 1000-3000. The relatively low values of the Q of ALN-based resonators are a consequence of material losses, which are specifically related to metal electrodes that are placed directly on the PE material. As far as the value of the product $f_0 \cdot Q$ (on the scale of 10^{12}) is concerned, LBARs in the form of an AlN ring with a lateral contour mode and LFE (SAW-BAW) resonators [8-10] have a prominent place among PE resonators. For example, the Q factor of SAW-BAW MEMS resonators with the resonance frequency of 843 MHz – 1.64 GHz, manufactured using the CMOS-compatible process, is up to 2200 in air [8]. The second lateral resonator [11], monolithically integrated with CMOS circuits, has f_0=1.01 GHz, and Q around 7000 in air.

Capacitive transduction influences the mechanical resonance frequency of a resonator through the effect of spring constant softening [12-14]. Namely, in capacitive MEMS resonators, along with the mechanical component, the effective stiffness has an electrical component (which depends on the DC-bias voltage, resonator-to-electrode gap spacing, g, the electrode overlap area, A_e, and the permittivity of the dielectric which fills the gap, ε_d). That is why the overall resonance frequency is different from the mechanical resonance frequency and is determined not only by the dimensions and the material parameters of the resonant structure, but also by the parameters V_p, g, A_e and ε_d. Capacitive MEMS resonators generally have higher Q than piezoelectric ones (because in piezoelectric resonators lossy metallic electrodes are deposited on top of the resonant structure). The Q factor of capacitive resonators that oscillate in bulk modes is greater than that in flexural resonators of the same resonance frequency due to lower energy loss (clamping loss, dissipation due to the surrounding medium, due to surface defects, thermoelastic effect) [15, 16]. The Q factor of capacitive bulk mode resonators remains at its maximum at higher values of pressure (i.e. $Q>10^5$ at pressures of $\sim 10^4$ Pa [17]) in comparison to

flexural ones, thus vacuum-packaging of certain types of resonators oscillating in bulk modes is not necessary in order to achieve a greater Q. However, there are other effects of gas presence in the environment (e.g. resonance frequency drift and fluctuations) that influence the choice of operating conditions and resonator packaging.

Fig. 3 shows the values of $f_0 \cdot Q$ reported in the literature for some of the realized capacitive MEMS resonators, for which we also show the values of the resonance frequency and the Q factor [14, 16-31]. This diagram can be used for the comparison of the performance of RF MEMS resonators and quartz resonators. It can be observed that $f_0 \cdot Q$ values corresponding to the best available quartz resonators are already reached by MEMS structures. Also, MEMS resonators go far beyond conventional CMOS (LC) resonators in terms of the presented parameters.

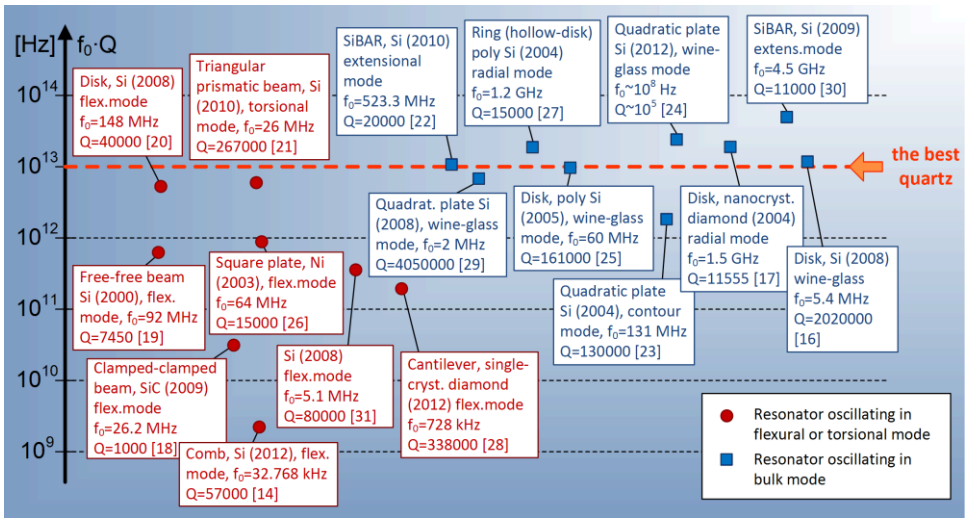

Fig. 3 Values of $f_0 \cdot Q$ reported in the literature for some of the realized capacitive MEMS resonators.

Capacitive resonators can be completely fabricated using materials that are compatible with silicon IC technologies, making them suitable for monolithic integration with transistor circuits. Although the highest level of integration is achieved by fabricating a resonator on the same chip with CMOS circuitry [32], which means that the fabrication of the resonator is embedded in an existing CMOS flow (it either precedes CMOS processing steps or is performed between them), it almost always implies degradation of the performance of either CMOS circuits or the resonator. The most convenient method of monolithic integration is the post-CMOS integration (or above-CMOS), in which the MEMS processing is done on top of prefabricated CMOS layers. In that case, the MEMS and CMOS processing steps are optimized and the mutual influence is minimized. However, then the temperature at which MEMS processing steps are performed is limited to 450°C, which influences the choice of resonator material [3]. For example, SiGe and Ni can be processed using low temperature techniques in order to fabricate resonators.

PE materials are not standard for Si technologies, which makes the integration of PE MEMS resonators with ICs difficult, with the exception of the resonator with an AlN layer. MEMS technology can be used for the fabrication of PE thin films. Sputtered AlN thin films can be processed below 450°C and they are therefore suitable for the integration of MEMS resonators on top of CMOS circuitry. Recent technological advances allow for the integration of PE resonators with CMOS circuits on the same chip [6]. For example, the SAW resonator (Q below 500) fabricated by combining a standard 0.6 μm CMOS processes and MEMS technology [33] is monolithically integrated on Si with active CMOS circuits. Over a period spanning more than a decade, great attention has been dedicated to the integration of FBAR with a CMOS circuits [34-37]. FBAR filters and duplexers are suitable for hybrid integration within the MCM (Multi-Chip Module). The monolithic FBAR-CMOS integration is more complicated to perform than the integration of MEMS SAW resonators and CMOS. Monolithically integrated 2 GHz FBAR on Si, described in [35], has Q=780, which is one of better results. Other AlN-based GHz FBAR resonator fabricated on top of a BiCMOS circuitry is presented in [38]. LBARs fabricated by processes compatible with Si IC technologies have better performance than CMOS-compatible FBARs. An example for this are the above-mentioned CMOS-compatible LBARs in the form of contour-mode oscillating AlN rings and LFERs, suitable e.g. for post-CMOS integrated on-chip direct GHz frequency synthesis in reconfigurable multiband wireless communications [9-11, 39].

However, it should be pointed out that though the MEMS-CMOS monolithic integration is desirable in terms of miniaturization, it may not be the best solution in terms of cost.

MEMS resonators operating in modes in which f_0 depends on lateral dimensions of a resonant structure (most of the capacitive bulk modes, SAW, LBAR) are suitable for realization of monolithically integrated RF filter banks, which consists of a large number of resonators with different resonant frequencies. Switches are commonly used for the selection of filters from a filter bank. Due to the simple filter selection (without switches that cause attenuation), and fabrication compatibility with Si IC technologies, capacitive resonators with bulk oscillating modes enable the fabrication of RF filter banks with minimal dimensions and minimal energy loss, monolithically integrated with active CMOS circuits.

The change of the resonance frequency in MEMS resonators with temperature is a result of the temperature dependence of the Young modulus of elasticity, the thermal expansion of materials, and mechanical stress in the resonant structure due to different coefficients of thermal expansion of the resonant structure and structures surrounding it. The relative change in the resonance frequency in most MEMS resonators is a linear function of temperature, with a negative slope [40]. The temperature coefficient of frequency of a Si resonator is typically between –15 ppm/°C and –30 ppm/°C [40]. Temperature stability of the frequency of PE resonators fabricated using the AlN technology is about –25 ppm/°C [41]. These values are acceptable for the implementation of preselect RF filters and RF image-rejection filters, but not for oscillators in which temperature stabilization of frequency is necessary. Different methods for temperature compensation are used in MEMS resonators: at the level of fabrication process, resonator design or external circuits [42-48, 3]. For example, doping of silicon reduces the temperature-dependence of the modulus of elasticity [45, 46]. A greater temperature stability of frequency can be achieved by fabricating the resonator using a combination of materials whose thermal expansion

coefficients are different and/or whose temperature coefficients of the Young modulus are different, so that an appropriate design can ensure the elimination of individual effects of temperature changes [47]. The effective stiffness and, consequently, the resonance frequency can be varied in order to ensure temperature compensation [49]. This may be achieved e.g. by a mechanical deformation of the structure, using temperature-dependent mechanical stress [50]. The adjustment of the resonance frequency can be done by changing the gap between the electrode and the resonant structure [12], the electrode overlap area [13] or the DC bias voltage, which change the effective stiffness as a function of the temperature [48]. The frequency adjustment range in capacitive resonators is larger than in piezoelectric ones. The range of 8.4% has been achieved in capacitive resonators by means of integrated heaters [51]. In FBARs operating above 1 GHz tuning range of 1.47% is achieved by using the tuning voltage of 7V [52]). One of the temperature compensation methods using external circuits is based on the temperature-dependent frequency synthesis. By applying various methods of compensation or their combination in MEMS resonators the temperature variation of the frequency is reduced to the value of 0.1-300 ppm in the temperature range between 60 K and 200 K [3]. In commercial MEMS oscillators (SiTime Inc.), the temperature compensation is achieved using digital techniques (a temperature sensor and an external CMOS circuit are used) [53].

Long-term frequency drift (i.e. frequency aging) of MEMS resonators of the order of ppm/year is observed [54], and it can be as low as 1 ppm/year [53, 55] which is better than that of a typical quartz resonator. The resonance frequency aging depends on the hermeticity of the resonator package.

The resonance frequency of EM resonators changes with pressure variations due to various effects. In quartz resonators, the influence of pressure on the modulus of elasticity dominates, due to which the resonance frequency increases linearly with the increase of pressure [41]. The resonance frequency of MEMS resonators decreases with increasing pressure, probably due to adsorption (binding) of the particles of surrounding gases onto the surface of the resonator. This effect is more pronounced in resonators of smaller size and mass.

The value of the equivalent series resistance (also called motional resistance), R_m, is important for the coupling of a resonator with other RF circuits. It should be low enough for the appropriate matching to the impedance of conventional RF circuits, which is typically 50 Ω. In filters, the signal attenuation in the passband is smaller at lower values of series resistance. In oscillators, the necessary amplification depends on R_m. Lower values of a resonator's series resistance in oscillators enable the amplifier gain to be lower, leading, consequently to lower power consumption. At lower R_m the output power is higher. Higher R_m values challenge the fulfillment of the requirements for starting and maintaining of oscillations [3], and increase the oscillator's phase noise.

Capacitive resonators typically have R_m of the order of 1-100 kΩ (regardless of the resonance frequency [3]), which can be a problem for coupling the resonators with antennae or other RF devices. For example, a flexural resonator (f_0=5.1 MHz, Q=80000) presented in [31] has R_m=35 kΩ; the Si resonator oscillating in flexural mode (f_0=1 MHz, Q=1000), described in [56], has a relatively small value of motional resistance (340 Ω), whereas the flexural Si resonator (f_0=14 MHz, Q=1500) from [57] has an extremely high value (1 MΩ). A Si square wine-glass mode resonator [29] has R_m=10 kΩ (f_0=2 MHz, Q=$4.05\cdot10^6$). Motional resistance of a quadratic Si plate resonator oscillating in the

contour mode (f_0=1.31 MHz, Q=130000) is 4.47 kΩ [23]. The resistance of a Si bulk-mode resonator in the form of a disk (2.1 kΩ, f_0=24 MHz, Q=53000) [58] is of the same order of magnitude, as well as that of the 145 MHz resonator (2.4 kΩ) [59]. Si bulk-mode resonators presented in [60] (f_0=13 MHz, Q=10^5) and [61] (f_0=60 MHz, Q=6200) have relatively small values of R_m, amounting to 500 Ω and 966 Ω, respectively. The bulk mode ring resonator described in [62] has R_m=200 kΩ (f_0=1.95 GHz, Q=8000). The reason for the high resistance values is in the nature of the electrostatic transduction mechanism in which a low intensity force is generated and used for actuation. There are several ways to reduce R_m: by using a higher bias voltage, by reducing the distance between the actuation/detection electrode and the resonant structure, by changing the resonator design (ensuring a greater overlap surface area of electrodes in capacitive transducers), by using several mechanically coupled resonators in parallel, etc.

PE resonators have lower motional resistance compared to capacitive ones similar in shape and size (due to a higher EM coupling coefficient). In addition, the value of the impedance in PE resonators decreases with the increase of f_0. FBARs have lower motional resistance than LBARs at the same electrode surface area (in FBARs, it is easy to achieve the R_m of 50 Ω). However, low R_m values have also been achieved in lateral PE resonators. For example, the R_m of AlN contour-mode ring-shaped resonators (f_0 in the range 223–656 MHz) is between 56 Ω and 205 Ω [9]. In LBARs in the form of a circular ring, the series resistance depends on the mean radius, whereas in square ring LBARs it depends on the mean side length of the basis, so by varying of those dimensions R_m can be adjusted without changing the resonant frequency, which is determined by the width of the ring. For example, a CMOS-compatible LFER (f_0=1.01 GHz) has R_m≈150 Ω [11, 39].

When the amplitude of oscillation becomes comparable with the characteristic dimension of the resonant structure in PE resonators or with the distance between the electrodes of capacitive resonators, the EM coupling coefficient and the effective stiffness of the resonator start to depend on the deformation, i.e. on the amplitude of the alternating actuation voltage and the resonator begins to work in a nonlinear regime [18, 63]. Nonlinear effects are a consequence of material nonlinearities, electromechanical coupling, or they have a different mechanical origin. Generally, when stress and strain reach a certain value, a linear relationship between them ceases to exist and the resonator stiffness constant becomes a function of stress and strain. In PE resonators, piezoelectric coefficients begin to non-linearly depend on strain. In capacitive resonators the nonlinear behavior is partly a direct consequence of a nonlinear relationship between the capacitance and the change in the distance between the electrodes. In addition, at high power levels parasitic modes can be excited along with the desired mode of oscillation. Nonlinear effects limit the maximum amplitude of oscillation, i.e. the maximum signal power at which the resonator operates in the linear regime. However, it is desirable that the amplitude of oscillation be as high as possible, i.e. that the resonator be capable of handling high power levels (for example, in order to reduce the oscillator phase noise). The power handling capability of MEMS resonators is lower than that of quartz resonators. For example, in flexural MEMS resonators, it is of the order of 1 μW, while in quartz resonators it is 100 times greater [18]. MEMS resonators with a higher stiffness can be driven by higher power levels while operating in the linear regime (non-linear effects are less pronounced); accordingly, the resonators which oscillate in bulk modes are better in this respect than flexural ones (for

example, maximal power may be of the order of 1 mW). Because of the higher Q factor and higher resonance frequencies compared to flexural resonators, capacitive resonators with bulk oscillation modes are more suitable for realization of filters and frequency synthesis in wireless transceivers. A smaller distance between the electrodes of capacitive transducers and higher voltage V_p lead to the increase of non-linearity and reduce the power handling capability. Capacitive resonators operate with a higher signal power in the linear regime if the overlap surface area of the electrodes is larger. Resonators with the PE transduction mechanism are more linear and have a better power handling capability (FBAR up to the order of 1 W). In MEMS resonators, a higher output signal power can be obtained using mechanically coupled parallel resonator arrays [64].

Based on the achieved parameter values, dimensions and CMOS compatibility, RF MEMS resonators are considered as a solution for realization of fully integrated RF systems. However, the potential of RF MEMS resonators for applications in wireless communications has not been sufficiently exploited yet. In the case of capacitive resonators, remaining problems that prevent wider practical application are high motional resistance and insufficient power handling, while in the case of high f_0 PE resonators it is a low Q (limited to several thousand). Nevertheless, significant results achieved after the year 2000 (especially in terms of better temperature stability, better long-term stability, improved packaging) have enabled the commercialization of both PE and capacitive MEMS resonators. An example of a commercial product is *Agilent's* FBAR filter from 2001. This is the first RF MEMS component that appeared on the market. FBAR filters have better performance (a higher Q factor, lower insertion loss, better selectivity, better temperature stability, the ability to work with higher RF powers - greater than 1 W) than conventional SAW filters at frequencies around 2 GHz and above. MEMS BAW (FBAR) resonators find the main application in mobile terminals, where they have replaced traditional duplexers, which are bulky non-integrated components. They are also used in bandpass filters, which are traditionally realized using conventional off-chip SAW components of larger dimensions. For example, by using FBAR components in mobile terminals instead of two SAW filters that are traditionally used for PCS bands 1850-1880 MHz and 1880-1910 MHz, the area needed for the transmission filter is reduced by 90%, and so is the realization cost. FBAR duplexers and filters are currently the only novel PE frequency selective components that meet all the required specifications of wireless standards and enable the miniaturization of the RF part of the transceivers of *multiband multimode* mobile terminals. The AlN FBAR resonator manufactured by *Avago Technologies* is the most successful MEMS resonator in the past decade [8]. Capacitive MEMS resonators that can be used instead of quartz resonators have also become commercially available (Discera, SiTime). The first silicon MEMS oscillator manufactured by Discera appeared in 2003. Its resonant structure is in the form of a cantilever, with dimensions of $30 \times 8\ \mu m^2$ and a resonance frequency of 19.2 MHz. The following year, the same manufacturer presented the first integrated MEMS tunable oscillator with a nominal frequency of 1.6 GHz, intended to be used as a voltage controlled oscillator of the local oscillator in transceivers of mobile terminals; however, it is not commercially available. In 2006, the first SiTime MEMS oscillators with a resonant structure in the shape of a square ring oscillating in the flexural mode appeared in the market. Commercially available is also a SiTime resonator with a resonace frequency of 5 MHz (Q=80000, V_p=1.8-4.6 V, long-term frequency stability 0.5 ppm/year, $800 \times 600 \times 150\ \mu m^3$ in size), fabricated on Si. A Si

MEMS chip is placed on a CMOS chip that contains amplifier circuits, circuits for temperature compensation and programmable memory. The dimensions of the packaging that contains both chips are $2 \times 1.6 \times 0.25\,\mathrm{mm}^3$ and this is currently the smallest programmable oscillator.

And what are the future needs? The development of MEMS resonators with f_0~1 GHz and $Q>10^4$ would enable implementation of new and compact multiband multistandard transceiver architectures (e.g. direct channel selection at the RF stage) [65]. Frequency references in the GHz range are also desirable in future wireless communications and other high-speed electronic systems. Although the possibility of fabrication of monolithically integrated MEMS resonator arrays of different resonance frequencies is very significant for multiband transceivers, enabling versatility and reconfigurability on a small surface, the ultimate objective in that sense are the resonators whose parameters are adjustable in a wide range, resulting in a significant reduction in the number of necessary components. Therefore, high-Q resonators oscillating at GHz frequencies and tunability of the resonance frequency are highly needed in future systems. In the next subsection the means for achieving these goals will be considered.

2.2. Achieving GHz resonance frequencies and the resonance frequency tuning

In order to achieve the resonance frequency of a mechanical structure in GHz range one has to choose appropriate geometry, dimensions and the material of the structure. The analysis will be performed for a doubly clamped beam resonator, since it is commonly used as a model structure in theoretic considerations. From the expression for the mechanical resonance frequency of the clamped-clamped beam oscillating in the first flexural mode, $f_0=1.03(h/L^2)(E/\rho)^{1/2}$, it is obvious that the resonance frequency will be higher if a structure is made of a material with a high E/ρ ratio (E is the material's Young modulus, ρ is its density) and also if the geometric parameter h/L^2 (h is the beam thickness, and L is its length) is high. Fig. 4 shows the calculated dependence of the resonant frequency on h/L^2 for the beams made of different materials commonly used in MEMS and characterized by the ratio E/ρ. This diagram is created based on the diagram in Ref. [66]. It leads to the conclusion about the values of the h/L^2 ratio at which GHz frequencies can be achieved with a beam made of a certain material. The calculation results (according to the expression for f_0 given above) suggest that resonators with GHz fundamental resonance frequencies have nanometer dimensions, and they are, therefore, fabricated using NEMS technologies.

In a majority of MEMS resonators realized so far, resonance frequency tuning is implemented in order to compensate temperature or fabrication process variations of the resonator parameters. Several frequency-tuning methods have been reported as mentioned before. However, tunable RF components for multiband transceivers require a much greater frequency tuning range compared to both temperature and process variation compensation. Mechanical tuning methods based on the change of the resonator's effective spring constant can yield a high tuning range without significant degradation of the Q factor, and are simple for implementation. Resonators with a high f_0 due to a high mechanical stiffness (oscillating in bulk modes) have a lower tunability than flexural resonators. One of the methods for frequency tuning through the change of the effective spring constant is based on the application of mechanical tension, i.e. tensile strain on the resonant structure. For example,

the resonant structure can be exposed to mechanical stress by using electrothermal actuators (they require a significant amount of additional surface area), by utilizing a more compact capacitive tuning in which the structure deforms under the influence of electrostatic force, or by some other mechanism. We analyze the resonance frequency dependence on mechanical tension in the case of a clamped-clamped beam, in order to quantitatively estimate the capabilities of the method in terms of both the tuning range and the influence of the resonator's parameters on the tuning range.

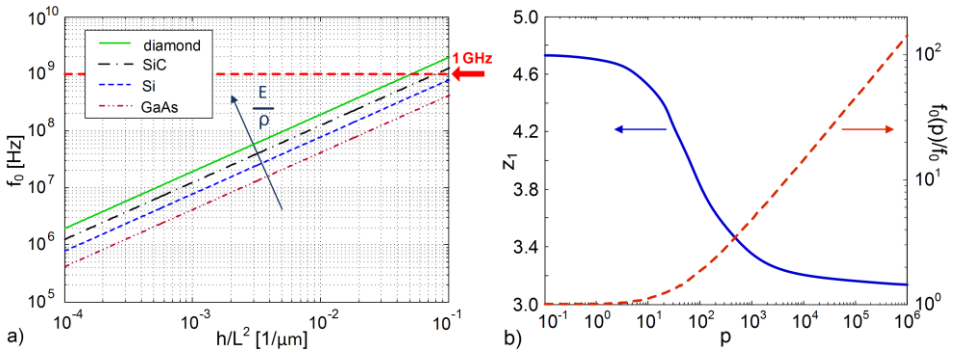

Fig. 4 Doubly clamped beam resonator oscillating in the first flexural mode: a) The dependence of the resonance frequency on the geometrical parameter h/L^2 (h is the beam thickness, and L is its length), for the beams made of different materials, characterized by the ratio E/ρ, b) Left axis: Dependence of the eigenvalue z_1 (determining the resonance frequency) on the tension dependent parameter p, Right axis: Ratio of the resonance frequency of an arbitrary beam under the tension and the resonance frequency in the absence of the tension, as a function of p (p=12$(L/h)^2\varepsilon$, ε is the uniaxial tensile strain).

The resonance frequency of the n-th flexural mode of a resonant structure in the shape of a double-clamped beam, under the tension N, is given as

$$f_{n0}(N) = f_{n0}(0)\frac{z_n^2(N)}{z_n^2(0)}\sqrt{1+\frac{p(N)}{z_n^2(N)}} = \frac{z_n^2(N)}{2\pi L^2}\sqrt{\frac{EI}{\rho wh}}\sqrt{1+\frac{p(N)}{z_n^2(N)}} \quad (1)$$

where $f_{n0}(0)$ is the beam's resonance frequency in the absence of the tension, $L\times w\times h$ are the beam's dimensions (length×width×thickness), E is the Young modulus, I is the moment of inertia ($I=wh^3/12$ for a beam with a rectangular cross-section), and the tension-dependent parameter p is

$$p(N) = NL^2/(EI) = 12(L/h)^2\varepsilon \quad (2)$$

In the above expression ε is the applied uniaxial strain. The equation that has to be solved [67] for z_n in order to obtain the resonance frequency of the n-th flexural mode of a double-clamped beam under tension, written in a convenient form, is

$$\cos(z_n)\cosh(z_n\sqrt{1+p/z_n^2}) - [p/(2z_n^2\sqrt{1+p/z_n^2})]\sin(z_n)\sinh(z_n\sqrt{1+p/z_n^2}) = 1 \quad (3)$$

This equation is solved for the first (fundamental) oscillation mode, considering three characteristic cases:

a) when p is low, i.e. $p \approx 0$, which corresponds to the absence of tension, Eq. (3) becomes

$$\cos(z_n)\cosh(z_n) = 1 \tag{4}$$

which for n=1 yields $z_1(0)$=4.73.

b) when p is high, thus $p/z_n^2 >> 1$, Eq. (3) is approximately

$$\sin(z_n - arctg(2z_n / \sqrt{p})) = 0 \tag{5}$$

and its solution corresponding to the first mode is $z_1 = \pi$.

c) for arbitrary p, Eq. (3) was solved numerically.

The obtained dependence $z_1(p)$ is shown graphically in Fig. 4b (the left axis). Based on it the frequency ratio $f_1(N)/f_1(0)$ is calculated as a function of the parameter p and shown in the same diagram (the right axis). (In the remaining text and diagrams the first mode resonance frequency will be denoted with f_0 instead of f_{10}.) This diagram gives a general insight into the amount of change of the resonance frequency of an arbitrary beam resonator oscillating in the given mode, attainable by applying an arbitrary tensile strain. For a resonator with a given L/h ratio and under a certain amount of strain, the frequency tuning ratio can be obtained based on Eq. (2). For example, assuming the maximal strain of 1% (corresponding to the yield strength of common semiconductor materials used in MEMS), for MEMS resonators with the ratio L/h=60 the parameter p=432, so the maximum tuning ratio of 3.3 is obtained from the diagram.

The diagram in Fig. 5a shows the dependence of the first flexural mode resonance frequency of doubly clamped beam resonators (L/h=60), made of various semiconductor materials commonly used in MEMS, on the applied uniaxial tensile strain. This dependence is obtained by applying the presented theory. Two distinct regions can be observed in the diagram. In the first region, which corresponds to low values of ε ($p/z_n^2 << 1$, so Eq. (4) is valid), the resonance frequency is practically independent of tension. This is the bending-dominated resonant frequency region. In the second region the increase of the resonant frequency with the applied strain can be clearly seen, and also the mentioned ratio $f_0(\varepsilon)/f_0(0)$ of 3.3, that corresponds to ε=1%. As the tension increases, it begins to dominantly determine the resonance frequency ($p/z_n^2 >> 1$), so this region is called the tension-dominated resonance frequency region. Also, it can be concluded from the same diagram that the ratio $f_0(\varepsilon)/f_0(0)$ does not depend on the parameters of the material. The dependence of the same ratio on ε is shown in Fig. 5b for three different values of L/h (20, 100 i 1000). The values of ε at which the resonance frequency is bending-dominated (or tension-dominated) depends on the ratio L/h. At higher L/h ratios lower ε values are required in order to attain a certain factor of the resonance frequency change, i.e. the same strain applied in a resonator of a higher L/h ratio yields a higher $f_0(\varepsilon)/f_0(0)$ ratio. For fixed L/h, the maximum achievable resonance frequency depends on the maximal possible strain (it depends on the resonator's material properties and the maximum value of the control voltage in the given application).

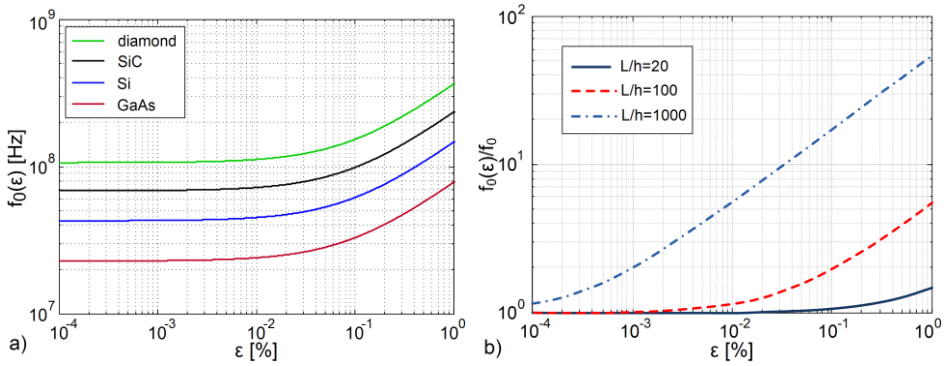

Fig. 5 Doubly clamped beam resonators oscillating in the first flexural mode: a) The dependence of the resonance frequency of beams (L/h=60) made of various semiconductor materials commonly used in MEMS, on the applied uniaxial tensile strain, b) The dependence of the ratio of the resonance frequency of a beam under the tension (i.e. axial strain) and the resonance frequency in the absence of the tension, on strain, for three different values of L/h.

Based on the presented analysis and results from the literature, the following conclusions can be made:

1. in order to achieve nominal resonance frequencies in the GHz range, the resonator needs to be made of a material with high E/ρ ratio (i.e. the material should be stiff and/or light); also, the resonant structure needs to be of nanometer dimensions (the domain of NEMS technologies),
2. for a wide frequency tuning range to be achieved by application of tensile strain, the material needs to have a high yield strength (i.e. to withstand a high strain); it is also necessary for the L/h ratio to be as high as possible,
3. high resonance frequencies of MEMS resonators are typically achieved in structures of high mechanical stiffness, which makes frequency tuning difficult. NEMS resonators, however, achieve high resonance frequencies while having the mechanical compliance needed for tunability [68].

2.3. Transition from MEMS to NEMS resonators. RF MEMS/NEMS dimensions scalling - Challenges

Nanoelectromechanical (NEMS) systems contain mechanical features whose at least one dimension is under 1 micrometer. Since the year 2000 a significant advance has been achieved in the development of NEMS resonators. Due to unique mechanical properties, NEMS resonators provide a promising basis for future ultrafast communication systems, highly-sensitive force and mass sensors, biomedicine etc.

A majority of NEMS resonators is in the shape of a nanoscale beam (doubly-clamped, cantilever or free-standing) made of Si or SiC, that oscillates in response to an applied external force [66, 69-72]. Their length is typically between 1-20 μm, while the thickness and width are smaller than 1 μm. The effective mass of NEMS is usually 10^{-14} g, and typical resonance frequencies are in the range between 1 MHz and 10 GHz [70], while the dissipated power can be as low as 10^{-17} W.

The first RF Si resonator of nanoscale dimensions (7.7 μm × 330 nm × 800 nm, beam shape), reported in 1996, had the fundamental resonance frequency around 70 MHz and Q=1.8·10^4 [69]. Later the silicon NEMS beam resonator fundamental frequency of 380 MHz was reached, with Q of the order of 1000 at room temperatures [73]. First NEMS resonators whose resonance frequency exceeded 1 GHz were SiC beams [74]. Dimensions of one of them, with the resonance frequency of 1.029 GHz, are 1.1 μm × 120 nm × 75 nm, and Q~10^4. Other materials typical for MEMS, such as gallium arsenide, silicon nitride, aluminum nitride and nanocrystalline diamond, are also used for fabrication of NEMS beam resonators with similar values of Q as previously mentioned, and f_0 being in the range from the order of 10 MHz to the order of 100 MHz [75, 76]. For example, a doubly clamped nanobeam AlN resonator (4 μm × 900 nm × 320 nm) oscillating in flexural mode has the resonance frequency of 78.2 MHz, and Q=670 at room temperature [77]. Metallic (Au, Pt, Al, Ti) NEMS resonators were also demonstrated, having fundamental resonance frequencies of the order of 10 – 100 MHz, and Q of the order of 1000 at the temperature of 4 K [78, 79]. Nanostructures of a high aspect ratio (defined as the ratio L/h or L/d, where d is a structure diameter) are called nanowires. They can be made of Si, SiC, Au, Ag, Pt, Ge, ZnO, GaAs, SiN etc. [78-83].

Some of techniques for fabrication of NEMS resonators are inherited from MEMS. However, the transition from micro- to nanoscale often implies qualitatively new technological solutions. Different methods exist for fabrication of NEMS/nanowire resonators, and can be divided into the following categories: top-down, bottom-up and hybrid methods. In top-down methods NEMS devices are made of bulk materials or thin films that are patterned by lithography and etching to create fully released structures such as clamped beams and cantilevers. Top-down methods are e.g. those based on standard electron beam lithography (EBL), superlattice nanowire pattern-transfer (SNAP), nanoimprint lithography (NIL) or stencil lithography. Top-down methods typically provide a high level of control regarding the design and geometry of the resonator. By using EBL very high aspect ratios of NEMS structures are achieved, such as L/h~250 in 20-25 nm thick SiC nanowires presented in [81]. This method enables fabrication of nanowires using different materials such as Si, GaAs, SiN etc. Nanowires made of Au, Cr, Al, Ti, Nb, Pt or Ni by using SNAP method are reported. One of them is a suspended Pt nanowire with a diameter of 20 nm and a length of 0.75 μm (a diameter as small as 8 nm is possible) [80]. NIL offers high resolution (5 nm) and also high-volume fabrication. Metallic nanowires can be fabricated by using wafer-scale stencil lithography. In [82] 70 nm thin Al nanowires, 5 μm long, fabricated by using this method are presented. Bottom-up methods include, for example, synthesis of Si, SiC, GaN, ZnO nanowires by vapor-liquid-solid (VLS) growth. Problem of bottom-up methods in general is the control of nanowire length, diameter and spatial distribution. Another disadvantage of these methods is their low efficiency. Hybrid top-down/bottom-up methods include, for example, integration of Si nanowires synthesis into device fabrication [83]. These methods enable better control of nanowire dimensions. Si nanowires of a 50-150 nm diameter, about 2 μm in length, fabricated by using a hybrid method, are presented in [71]. Among them are a metalized Si nanowire with a resonance frequency about 200 MHz and Q≈2500 (measured in high vacuum at cryogenic temperatures), whose resistance is matched to 50 Ω, a 80 MHz non-metalized Si nanowire with Q=13100, and a non-metalized Si nanowire with f_0=215 MHz and Q=5750 (the

resistance of the latter two is of order of 10-100 kΩ). It can be concluded that the product $f_0 \cdot Q$ of the order of 10^{12} is achieved in nanowire resonators.

There are several methods of actuation and detection of motion in NEMS resonators: electrostatic, optical (e.g. free-space or fiber-optical interferometry), piezoelectric, magnetomotive/electromotive, piezoresistive, methods based on single electron transistors (SET), atomic point contact (limited to resonators made of conductive materials that do not form surface oxides), photonic transduction etc. However, not all the mentioned methods are equally suitable for applications requiring a compact actuation and detection system (preferably on a chip), for resonators of extremely small dimensions or those made of arbitrary materials. For example, magnetomotive transduction is often the right choice for both drive and detection of motion of very small structures oscillating at extremely high frequencies. However, its significant limitation is that it requires a strong magnetic field (1–16 T) produced by a superconducting magnet. Such a strong field also causes circuit loading and renders the setup large and expensive. Purely capacitive transduction methods suffer from very low signal levels and parasitic coupling at very high frequencies. Optical transduction cannot be realized on-chip, and its sensitivity decreases as the resonator size scales down, because the diameter of the focused beam is limited from below by diffraction (this limitation can be overcome by using waveguides of a submicron cross-section, located on the substrate near the resonator). Photonic method implies significant fabrication difficulties for dimensions of the order of 10 nm and below. Promising results have been reported regarding optical multiplexing techniques. The transduction efficiency of the piezoelectric method is very high and it is extensively used in bulk mode MEMS resonators. However, the method is less convenient for small structures as the crystalline structure must be maintained for a material to be piezoelectric, thus limiting the lowest possible device thickness. Nevertheless, both NEMS cantilevers and doubly-clamped beams have been successfully demonstrated with PE layers as thin as 100 nm, proving that PE layers can be used as efficient nanoscale transducers [77]. Intrinsic amplification mechanisms such as transistor-based charge modulation are promising at room temperatures. Pronounced piezoresistive effect in doped Si nanowires due to longitudinal strain enables integrated piezoresistive self-sensing of strain or displacement (a nanowire without patterned piezoresistor loop is a transducer) [84]. Some other methods (based on SET or superconductive microwave cavity) are used only at low temperatures [85], and are difficult to implement. One of interesting new all-on-chip solutions applicable at room temperature is, for example, a self-transducing NEMS system based on the cointegration of a finFET transistor and a suspended doubly-clamped beam silicon resonator [86]. In this example electrostatic actuation and transistor-based detection of the resonator motion are used.

There are significant benefits of scaling down the dimensions, such as high speed operation, higher resonance frequencies, higher component density and better integration. However, apart from the mentioned features of NEMS components, which are a result of miniaturization, and beneficial in high-frequency signal processing and sensing applications, there are problems that remain to be solved on both theoretic and experimental level. The studies in the field of NEMS are at the forefront of physical and engineering sciences. Most developments in this field are currently confined to theoretic models, simulations and laboratory experiments, with NEMS components in a prototype stage, at best.

Some solutions used in MEMS do not scale well into the NEMS domain. Apart from technological issues regarding reproducibility and control of surface and bulk properties of extremely small structures, remaining issues include efficient energy conversion mechanisms and coupling between NEMS and other components and circuits. The small size of NEMS typically results in a small motional signal. In spite of many different transduction methods applied in NEMS resonators so far, inducing resonator motion and detecting of weak mechanical signals at very high oscillation frequencies, at room temperature and with low power dissipation remain challenging, especially if a compact solution, such as a system-on-chip, is required. Small motional signal can easily be overwhelmed by parasitic coupling or background noise. As the dimensions decrease, so does the signal-to-noise ratio. There are also problems with energy loss at clamping sites (clamping loss), which increases with f_0, as well as with surface losses and other effects leading to the increase in energy dissipation, and, consequently, the Q factor decrease. Therefore, there are limits to the reduction of device size. Q of NEMS resonators can reach thousands, even tens of thousands, but, except in rare cases, such Q values have been reached only at temperatures below 25 K. A SiN 50 nm thick square membrane with the fundamental resonance frequency of 133 kHz is an example of a NEMS resonator with Q of the order of 10^6 at the room temperature [87]. However, attaining a high fundamental resonance frequency without decreasing the Q value is the remaining problem in NEMS development. As in MEMS, solutions are also needed for reduction of the series resistance of NEMS resonators and improvement of their power handling.

From the theoretical standpoint, it is important to analyze the applicability of the continuum approach to the calculation of mechanical characteristics of an extremely small resonator.

Reduction of the noise caused by physical effects that become pronounced as the dimensions decrease is another important task which requires both theoretic and experimental research. In MEMS, and especially in NEMS resonators, additional noise generating mechanisms exist that are characteristic for structures of small dimensions and mass, and high surface-to-volume ratio. It is therefore necessary to investigate their influence on the resonator performance as a function of dimensions of the structures and the operating conditions. In Section 3, by analyzing the adsorption-desorption (AD) noise that becomes prominent as the dimensions and mass of the components decrease, we contribute to the theory of noise in MEMS and NEMS resonators, and subsequently to the theory of phase noise in oscillators using RF MEMS/NEMS resonators as frequency determining elements.

2.4. RF NEMS resonators based on 2D crystals

Recent years have seen increasing interest in NEMS that utilize carbon nanostructures, such as one-dimensional (1D) nanotubes or two-dimensional (2D) beams or membranes, as building blocks. These structures are based on graphene, a planar sheet of carbon atoms arranged in a honeycomb lattice. Graphene structures, consisting of one or a few of atomic layers, are intrinsically nanoscale. Since the carbon-based nanostructures emerged, a continued miniaturization of resonant NEMS has advanced into atomically thin 2D or 1D NEMS.

Graphene has high 2D elastic stiffness (2D Young's modulus E_{2D}=340 N/m, corresponding to E=1 TPa reduced to a single atomic layer) and high breaking strain (25%), which exceed the values for any of the thin-film materials currently used for NEMS. It also has a low mass (ρ_{2D}=7.4·10^{-7} kg/m^2) and a high E/ρ ratio. The strength of carbon-carbon bond makes graphene quite flexible. Being atomically thick, graphene structures have extremely high L/h ratio. These characteristics imply that the conclusions 1-3 made at the end of Section 2.2 are in favor of graphene-based resonators as opposed to MEMS and NEMS resonators made of traditional materials: graphene structures can have high resonance frequencies which can be further increased and widely tuned by application of large strains. For example, for a graphene beam of 1 μm in length, and exposed to 1 % of strain, the parameter p (Eq. (2)) is about 10^6, which, according to the diagram in Fig. 4b yields the ratio of the resonance frequencies of stretched and unstretched beam as high as 10^2 (in typical MEMS resonators the ratio is 3.3, as stated earlier). Apart from that, graphene's charge-tunable conductance and large charge mobility allow the efficient electrical transduction of mechanical vibration to electrical signal. Thus, there is a growing interest in the development of graphene-based NEMS resonators.

In Fig. 6a a schematic diagram is given of a graphene doubly-clamped beam exposed to tensile strain. Fig. 6b shows the strain dependence of the first mode resonance frequencies of 1 μm and 2 μm long doubly-clamped graphene beams (obtained by using Eqs. (1)-(3)). It indicates that the resonance frequency can be increased by several orders of magnitude when stretching is applied, compared to the resonance frequency of the unstretched beam, which is a consequence of a high L/h ratio (L/h is about 3000 for a 1 μm long graphene beam). Because of that, GHz frequencies can be attained even when resonance frequencies of unstretched beams are in the MHz-range (typical for 2D resonators 1-5 μm long). As it can be seen by comparison of Figs. 5a and 6b, in atomically thin structures the values of ε above which the tension dominated resonance frequency region begins are significantly lower than in MEMS/NEMS resonators of a lower L/h ratio.

In the following text a short description will be given of two types of carbon (graphene) based resonators: carbon nanotube resonators and graphene (beam and membrane) resonators.

A carbon nanotube (CNT) is a hollow cylinder of covalently bonded carbon atoms. Depending on the number of graphene sheets that are rolled concentrically, such a structure can be a single-walled carbon nanotube (SWNT) or a multi-walled carbon nanotube (MWNT). The first successfully fabricated nanotubes were reported in 1991 [88]. Typically, the diameter of a SWNT is 1-2 nm, and the length is several micrometers (several millimeters long SWNTs have also been reported [89]). The diameter of MWNT is usually 2-25 nm, and its length is several tens of micrometers (they can be grown up to several centimeters in length [90]). Currently, these bottom-up structures are typically synthesized by chemical vapor deposition (CVD), using the catalyst-assisted method which enables obtaining of nanotubes that are defect-free or with a few defects only.

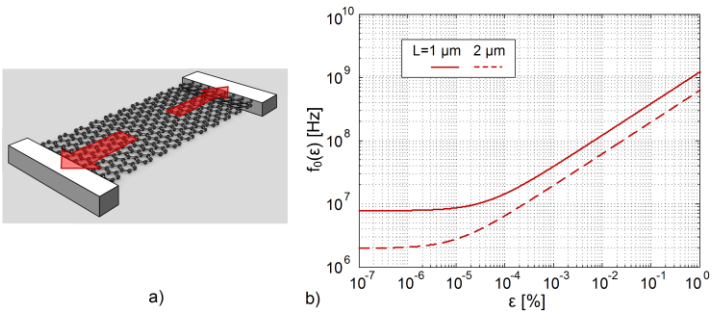

Fig. 6 a) Schematic representation of a 2D (graphene) beam resonator under tension, b) The strain dependence of the first mode resonance frequencies of 1 μm and 2 μm long doubly-clamped graphene beams.

The first nanotube resonator was made out of MWNT in 1999 [91]. Tunable SWNT and MWNT resonators have been reported in 2004 [92]. Method of actuation and detection of a nanotube resonator motion, suitable for realization on a single chip, is described in [92]. The actuation is achieved through the electrostatic interaction between the tube and the underneath gate electrode, while the detection rely on NTs transistor properties, i.e. on the change in the conductance of nanotube due to modulation of NT-gate capacitance, which is caused by vibration of the nanotube, and measured by using the frequency mixing technique. This method was applied in characterization of double-clamped SWNTs with the diameter of 1-4 nm, the length of 1.75-3 μm, the resonance frequency in the range of 5.1-333 MHz, and *Q*s of 50-100 (*Q*=100 corresponds to the NT with the lowest f_0, and *Q*=50 to the highest f_0 NT, measured in vacuum at room temperature) [93]. Nanotube resonators operating at the GHz range, potentially applicable in RF systems, have been demonstrated recently [94, 95]. Mechanical resonances as high as 39 GHz have been observed in carbon nanotube resonators [96]. Typical values of NT resonators' Q factor (from the order of 10 to the order of 100 at the room temperature) are lower than those of NEMS resonators made of conventional materials. For example, for a doubly-clamped SWNT of 3 μm in length and with f_0=26.1 MHz, Q factor about 90 is measured at room temperature and at the pressure of 10^{-4} Torr [97]. Detailed consideration of different dissipation mechanisms in NT resonators is performed in [98]. Lowering the temperature reduces dissipation, allowing for quality factors up to 2000 [99]. The highest reported *Q* in NTs exceeds 10^5 (SWNT, f_0=350 MHz), but it is obtained at as low a temperature as 25 mK, when tensile strain is applied [100]. Among the highest Q values (about 700) reported at room temperature and the pressure of 10^{-4} Torr is for a doubly-clamped SWNT (3 μm length, f_0≈83 MHz), and the increase of *Q* is attained by applying the parametric amplification concept [97]. The frequency of SWNT resonators presented in [97] is tuned by varying the gate voltage, which changes the electrostatic force, so both the stretching (i.e. the increase of tension) of the nanotube and the electrostatic interaction with the gate occur, changing the nanotube effective spring constant. At the tuning voltage of 10 V, the resonance frequency increase of as much as 200% (the spring hardening effect due to increased tension dominates the electrostatically induced spring softening effect) is reported. In [93], by varying the gate voltage from 2 V to 3.5 V the tension in

NT was changed, thus enabling the adjustment of the resonance frequency in the range 7-14 MHz. A tunable band-pass filter utilizing singly-clamped NT resonator is analyzed in [101]. The center frequency and the bandwidth of the filter are voltage-tunable: the increase of the frequency by over 100% is attainable by varying the tuning voltage from 0 V to 50 V, while the bandwidth simultaneously decreases by 50%.

Graphene was obtained for the first time by mechanical exfoliation from graphite [102]. Nowadays, graphene structures can be fabricated by a combination of top-down and bottom-up methods. Unlike NTs, graphene can be grown over large areas (using CVD or SiC annealing). Moreover, graphene can be patterned at the wafer scale by standard lithographic processes, compatible with other top-down processing techniques, which makes its integration with other components possible.

The first graphene electromechanical resonator was demonstrated in 2007 [103]. The motion of a suspended graphene sheet (in the form of a doubly-clamped beam) was actuated by using the laser-based optical method or electrical method, and for detection an interferometric method was applied. Subsequently, electrostatic excitation of mechanical vibrations combined with SPM (Scanning Probe Microscopy) detection was used for graphene resonators [104]. The electrical detection method, based on the change of conductivity of vibrating single-layer graphene due to the change of its distance from the gate, is described in [105], where the feasibility of actuating and detecting resonance on a single chip was confirmed.

Graphene resonators in the form of doubly-clamped beams have Q of the order of 10-100. For example, a single-layer graphene beam ($1100 \times 1930 \times 0.3$ nm^3) has f_0=70.5 MHz and Q=78, and a 15 nm thick multilayer graphene beam has f_0=42 MHz and Q=210, both at room temperature and pressure below 10^{-6} Torr [103]. A graphene resonator in the form of a circular membrane (4 μm in diameter) has f_0=52.19 MHz and Q=55 [68]. Drum-like graphene resonators of high Q factor are also reported; for example, the Q factor about 2400 is obtained at the room temperature and pressure lower than $6 \cdot 10^{-3}$ Torr for the membrane of 22.5 μm in diameter (f_0 about 4 MHz) [106]. In graphene resonators Q increases as the temperature decreases. As the temperature decreases to 50 K, the Q factor of beam resonators rises above 1000 [103], while at 5 K it can be as high as 10000 (f_0=130 MHz) [105]. Energy dissipation mechanisms that determine the Q factor value in graphene resonators are reviewed in detail in [98].

Due to a built-in tension, resonance frequencies of graphene resonators are higher than expected for structures of given dimensions and predicted by bending alone. The built-in tension originates from the fabrication process [103]. A typical built-in strain is of the order of 10^{-5}-10^{-4} [105].

A high tunability of graphene resonance with the applied gate voltage that induces tension in the resonant structure is observed [105]. The resonance frequency of a 3 μm wide and 1.1 μm long single-layer graphene beam increases from 30 MHz to 65 MHz as the gate voltage changes from 0 V to −7V [105]. The resonance frequency tunability as high as 400% is reached [105]. Tensile strain does not only increase the resonance frequency but can also significantly reduce dissipation (i.e. increase the Q factor) [98]. The increase of Q with the tensile strain is also observed in Si, SiN and GaAs NEMS resonators [98].

In Ref. [68], oscillators containing a graphene NEMS resonator are reported, whose frequency can be electrostatically tuned by as much as 14%. Self-sustaining mechanical vibrations are generated and transduced at the room temperature using simple electrical circuitry. The 52.2 MHz NEMS oscillator based on a graphene circular drum (4 μm in diameter) has Q=4015 at the room temperature. The graphene VCO, which is the first prototype device for RF applications based on graphene NEMS, presented in the same reference, shows promising performance. Also, in [68] experimental data pertinent to phase noise of graphene oscillators were presented for the first time.

Graphene resonators have more reproducible characteristics than NTs. Signal levels in graphene resonators are improved compared to those in NT resonators, due to the ability to fabricate micrometer-wide structures with higher conductance than that of one-dimensional nanotubes [105]. By exposing a micrometer-scale graphene resonator to strain, an increase in the resonance frequency (in GHz range) can be achieved without a decrease in the signal level, and the dynamic range also increases with the strain (since the amplitude at the onset of nonlinearity increases with strain). This is an advantage compared to top-down NEMS in which high resonance frequencies are achieved by reducing the resonator dimensions, which in turn causes a decrease of both the output signal magnitude and the amplitude at the onset of nonlinearity, also decreasing the dynamic range and making GHz-range transduction difficult [105].

In spite of the great potential of carbon nanotubes and graphene in resonator applications due to their extraordinary mechanical properties (enabling high resonance frequencies and high tunability), there is a number of issues that need to be addressed in order to enable practical applications. For example, integration of CNTs and control over their location on-chip make mass production of CNT-based NEMS devices difficult to achieve. Further research activities aim to provide simpler and more reproducible techniques for fabrication of ultraclean nanotubes, and exploration of frequency tuning mechanisms and nanotube nonlinear dynamics. The improvement of quality factors of both nanotube and graphene resonators is an important task. CNT and graphene structures have the largest surface-to-volume ratios, so surface effects become increasingly important to investigate. Noise generation mechanisms in these structures also require further investigation in order for their ultimate performances to be determined.

Also related to the subject of this paper are adsorbed mass fluctuations that generate the adsorption-desorption phase noise of resonators and oscillators. The extremely low mass of graphene structures, and their large surface-to-volume ratio make these resonators highly sensitive to added mass. Therefore, the properties of such structures are highly sensitive to the amount of adsorbates and its change [107]. Due to the high sensitivity to mass, stochastic adsorbed mass fluctuations could influence the fluctuations of graphene resonator parameters, i.e. the resonator total noise. There is not enough data in the literature about the effects of gas adsorption on mechanical and electrical parameters of graphene resonators and their oscillation, and therefore this topic requires further investigation.

3. PHASE NOISE IN RF MEMS/NEMS

Operation of MEMS and NEMS components (including RF) is based on the interaction between the mechanical and the electrical domain of the system. Thus, apart from the noises inherent to electrical and electronic devices (e.g. thermal (Johnson) noise, shot noise, generation-recombination (GR) noise, 1/f noise), generated in EM transducer circuits, amplifiers and other electronic parts of MEMS/NEMS systems, noise analysis in MEMS/NEMS has to include noise generating mechanisms in the mechanical domain [108]. Fundamental (internal) mechanical noises are the consequence of the stochastic nature of physical processes occurring inside the MEMS/NEMS component or at the interface between the mechanical structure and the environment, which result in stochastic fluctuations of displacement of a mechanical structure and/or of its mechanical resonance properties, thus causing fluctuations of the electrical output signal. Characteristic fundamental mechanical noises of MEMS/NEMS resonators are thermo-mechanical (TM) noise, noise due to temperature fluctuations (TF), and adsorption-desorption (AD) noise. Their contribution to the total noise increases and may become dominant as the dimensions, mass and displacement of mechanical structures decrease.

The short-term frequency stability, which is a significant parameter of MEMS/NEMS resonators, is determined by the phase noise. The oscillator phase noise, that degrades the signal transmission quality, originates from phase fluctuations caused by noise generation mechanisms in the oscillator's electronic circuit and also from the resonator noise [109]. The fundamental mechanical noises cause unavoidable stochastic fluctuations of the phase and frequency of a resonant structure oscillation and determine the lowest (fundamental) limit of the MEMS/NEMS resonator noise. Therefore, TM, TF and AD noise are considered as a measure of the MEMS/NEMS resonator ultimate performance. Although theoretical considerations of TM, TF and AD noise in MEMS/NEMS were published in the literature [108, 110-114], a need for more comprehensive models of noise in MEMS/NEMS resonators and oscillators still exists. Further in this section, theoretic models of AD noise in RF MEMS/NEMS EM resonators and of phase noise in MEMS/NEMS oscillators, presented in our papers [113, 115-123], will be briefly reviewed, and then the results of the quantitative analysis will be given.

3.1. Adsorption-Desorption noise in MEMS/NEMS resonators

In mechanical structures of micrometer or sub-micrometer dimensions and minuscule mass, whose displacement is in nanometer range, the effects of physical phenomena that are negligible in the macroscopic world become significant. Among such phenomena are adsorption and desorption of surrounding gases, that spontaneously and inevitably occur on surfaces of all solid bodies at temperatures higher than 0 K, and at pressures above 0 Pa. Stochastic nature of both the instantaneous adsorption and desorption rate results in stochastic fluctuations of the adsorbed particles number, $\Delta N(t)$, and consequently the total adsorbed mass fluctuates ($\Delta m(t)$) causing fluctuations of the mechanical resonance frequency of the MEMS/NEMS structure, $\Delta f(t)$, i.e. the resonator adsorption-desorption (AD) frequency and phase noise. The mean power of AD phase noise of a resonator in the bandwidth 1 Hz at the offset-frequency ν from the nominal frequency f_0, expressed in dBc/Hz, is [123]

$$L_R = 10\log(S_{\Delta f}(\nu)/(2\nu^2)) = 10\log((f_0/2m)^2 S_{\Delta m}(\nu)/(2\nu^2)) \tag{6}$$

where $S_{\Delta\nu}(\nu)$ is the power spectral density (PSD) of resonator AD frequency noise. Both these quantities are determined by the PSD of the adsorbed mass fluctuations, $S_{\Delta m}(\nu)$ (m is the resonator mass).

In order to perform the statistical analysis of AD processes by using the approach which is common for gain-loss processes (AD processes and generation-recombination (GR) processes belong to them), the equation(s) describing the change of the number of adsorbed gas particles in time is (are) shown in the general Langevin form

$$dN_i/dt = g_{ie}(N_1, N_2, \ldots, N_n) - r_{ie}(N_1, N_2, \ldots, N_n) + \xi_i \tag{7}$$

i=1,2,...n, valid for different types of AD processes. Here, $n\geq 1$ is the total number of gases in the resonator surroundings whose particles adsorb in a single layer on the resonator surface [113, 115-119], or the total number of adsorbed layers in the case of multilayer single-gas adsorption [120, 121]. The index "i" refers to i^{th} gas in a gas mixture, or to the particles in the ith adsorbing layer (which are not covered by $(i+1)^{\text{th}}$ layer). The equivalent rate of "generation" of adsorbed particles of the type i (i.e. of increase of their number) and the equivalent rate of their "recombination" (i.e. of decrease of their number), g_{ie} and r_{ie}, respectively, take into account the influences of all the processes relevant for the change of N_{i}, and their forms differ depending on the analyzed case of adsorption on the surface of micro/nanostructures: single gas single-layer adsorption [115], single-layer adsorption of an arbitrary number of gases [116, 117], adsorption in an arbitrary number of layers [120, 121], or adsorption coupled with mass transfer [118-119]). ξ_i is the stochastic source function.

For small fluctuations (ΔN_i) of the number of adsorbed particles around the corresponding equilibrium value (N_{iE}), so that $\Delta N_i << N_{iE}$, Eqs. (7) can be written in the matrix form

$$d([\Delta N_1\ \Delta N_2\ \ldots\ \Delta N_n]^T)/dt = -\mathbf{K}\cdot[\Delta N_1\ \Delta N_2\ \ldots\ \Delta N_n]^T + [\xi_1\ \xi_2\ \ldots\ \xi_n]^T \tag{8}$$

$$d(\Delta\mathbf{N})/dt = -\mathbf{K}\cdot\Delta\mathbf{N} + \boldsymbol{\xi} \tag{9}$$

where $\mathbf{K}$ is the $n\times n$ matrix of elements $K_{ij}=-(\partial g_{ie}/\partial N_j - \partial r_{ie}/\partial N_j)\big|_{\mathbf{N}=\mathbf{N}_{\text{E}}}$, $\mathbf{N}=[N_1\ N_2\ \ldots\ N_n]^{\text{T}}$, $\Delta\mathbf{N}=[\Delta N_1\ \Delta N_2\ \ldots\ \Delta N_n]^{\text{T}}$, and $\mathbf{N}_{\text{E}}=[N_{1\text{E}}\ N_{2\text{E}}\ \ldots\ N_{nE}]^{\text{T}}$ is the vector of steady-state values N_{iE}, which are obtained from the steady state conditions $g_{ie}(N_{1\text{E}},N_{2\text{E}},\ldots N_{nE})=r_{ie}(N_{1\text{E}},N_{2\text{E}},\ldots N_{nE})$. By performing Fourier analysis, a square $n\times n$ matrix $\mathbf{S}_{\Delta\text{N}2}(\omega)$ is obtained

$$\mathbf{S}_{\Delta\mathbf{N}^2}(\omega) = (\mathbf{K} + j\omega\mathbf{I})^{-1}\cdot\mathbf{S}_{\xi}\cdot(\mathbf{K}^{\mathbf{T}} - j\omega\mathbf{I})^{-1} \tag{10}$$

Its elements (i,j) are single-sided spectral and cross-spectral densities, $S_{\Delta Ni\Delta Nj*}(\nu)$ [119 Supplementary data]. According to the stochastic analysis of GR processes [124] and the analogy with AD processes, the PSD of the ith source function equals $S_{\xi i} = 4g_{ie}(N_{1E}, N_{2E}, \ldots, N_{nE})=4g_{ieE}$. Since ξ_i and ξ_j ($i\neq j$) are statistically independent, $\mathbf{S}_{\xi}$ is a diagonal $n\times n$ matrix of elements $S_{ii}=S_{\xi i}$. $\mathbf{I}$ is the unity $n\times n$ matrix, $\omega=2\pi\nu$.

The total fluctuation of the adsorbed mass is $\Delta m=M_1\Delta N_1+M_2\Delta N_2+\ldots+M_n\Delta N_n$, where M_i is the mass of a single particle of the type i (number of such particles at the surface is N_i). The PSD of adsorbed mass fluctuations is

$$S_{\Delta m,n}(\omega)=\mathbf{M}\cdot\mathbf{S}_{\Delta\mathbf{N}^2}(\omega)\cdot\mathbf{M}^{\mathbf{T}} \tag{11}$$

(M=[M_1 M_2 ... M_n]) and it can be expressed in the general form

$$S_{\Delta m,n}(\omega)=\left(\sum_{i=0}^{n-1}k_i\omega^{2i}\right)/\left(\prod_{i=1}^{n}(1+\omega^2\tau_i^2)\right) \tag{12}$$

Coefficients k_i and τ_i are obtained analytically for the given case of adsorption. The resonator AD phase and frequency noise are now obtained using Eq. (6), where $S_{\Delta m}(\nu)$ is given by Eq. (11) or (12).

In order to illustrate the applications of the presented approach, the results obtained for several characteristic cases of adsorption will be given. For example, in the case of single gas single-layer adsorption [113, 115, 123]

$$S_{\Delta m,1}(\nu)=\frac{4M_1^2g_{1e}(N_{1E})\tau_1^2}{1+(2\pi\nu)^2\tau_1^2} \tag{13}$$

where $\tau_1=1/K_{11}=-(\partial g_{1e}/\partial N_1-\partial r_{1e}/\partial N_1)^{-1}\big|_{N1=N1E}$, and N_{1E} is obtained from the steady state condition $g_{1e}(N_{1E})=r_{1e}(N_{1E})$. Considering the mass transfer process, the PSD of the adsorbed mass fluctuations for single gas single-layer case is also given by Eq. (13), with $\tau_{1,MT}=\tau_1(1+g_{1eE}RT/(Ak_mp))$ instead of τ_1 (p is the gas pressure, T is the temperature, A is the resonator surface area, and k_m is the mass transfer coefficient) [118]. Mass transfer processes of particles in a resonator chamber can influence the fluctuations of the number of adsorbed particles, especially for low-pressure (low-concentration) environments [118].

For the resonator operating in a two-gas atmosphere (the simplest case of multiple gas adsorption), the PSD of the mass adsorbed in a single layer is [116, 117]

$$S_{\Delta m,2}(\omega)=4\frac{\tau_1^2\tau_2^2}{\tau_z^2}\frac{(M_1^2g_{1eE}+M_2^2g_{2eE})(1+\omega^2\tau_z^2)}{(1+\omega^2\tau_1^2)(1+\omega^2\tau_2^2)} \tag{14}$$

where $\tau_{1,2}=2\{K_{11}+K_{22}\pm[(K_{11}+K_{22})^2-4(K_{11}K_{22}-K_{12}K_{21})]^{1/2}\}^{-1}$, $\tau_z=(M_1^2g_{1eE}+M_2^2g_{2eE})[(M_1K_{22}-M_2K_{21})^2g_{1eE}+(M_1K_{11}-M_2K_{12})^2g_{2eE})]^{-1}$. The same expression is valid in the case of two-layer adsorption, but $\tau_{1,2}$ and τ_z depend on different parameters because the functions g_{ie} and r_{ie} are different [120].

3.2. Phase noise in RF MEMS/NEMS oscillators

Oscillators, which produce continuous periodic signals from DC power, are important for modern communications systems, due to their versatile applications including timing references and frequency synthesizers. The effects of oscillator phase noise become increasingly destructive with the introduction of new wireless standards based on advanced modulation schemes [125], which makes modeling of RF oscillators phase

noise in modern wireless communication systems very useful. Therefore, the theory of phase noise is being constantly improved [125, 126].

A signal generated by a real oscillator can be expressed by $u(t)=A_0 2^{-1/2} e^{j2\pi f_0 t} e^{j\phi(t)}$, where A_0 is the amplitude (usually considered as constant [125]), f_0 is the carrier frequency, and $\phi(t)$ is the resulting stochastic fluctuation of the phase, caused by noise generating mechanisms in the oscillator constituting components. The spectrum of the signal $u(t)$ is located around the frequency $f=f_0$, and shaped by $\theta(t)=e^{j\phi(t)}$. Therefore, when considering only the spectrum shape, it is convenient to analyze the spectrum translated to the baseband, which is then the spectrum of $\theta(t)$. If the PSD of $\theta(t)$ is denoted with $S_\theta(\nu)$, the oscillator phase noise (expressed in dBc/Hz) is [125]

$$L_{osc}(\nu) = 10\log(S_\theta(\nu)) \tag{15}$$

(ν is the Fourier frequency). $S_\theta(\nu)$ is obtained by using the Wiener-Khinchin theorem

$$S_\theta(\nu) = \int_{-\infty}^{\infty} R_\theta(\tau) e^{-j2\pi\nu\tau} d\tau = \int_{-\infty}^{\infty} e^{-\sigma^2_{\Delta\varphi}(|\tau|)/2} e^{-j2\pi\nu\tau} d\tau \tag{16}$$

where $R_\theta(\tau)$ is the autocorrelation function of $\theta(t)$, and $\sigma^2_{\Delta\phi}(\tau)$ is the phase jitter variance (the variance of the phase increments) [125]. Since $\phi(t)$ is the integration result of stationary frequency noise, the variance $\sigma^2_{\Delta\phi}(\tau)$ is related to the PSD of frequency noise $S_{\Delta f}(\nu)$ according to the expression [125, 127]

$$\sigma^2_{\Delta\varphi}(\tau) = \int_{-\infty}^{\infty} S_{\Delta f}(\nu) \frac{\sin^2(\pi\nu\tau)}{(\pi\nu)^2} d\nu \tag{17}$$

Considering a MEMS oscillator consisting of a MEMS mechanical resonator (as a frequency selective element) and sustaining electronics, the total phase fluctuations are caused by noise generation mechanisms in the oscillator's electronic circuit, but also by the resonator mechanical frequency noises. Due to the noise induced by dissipation processes in a resonator and sustaining circuits (called the Brownian motion noise, or white noise), the phase undergoes diffusion process, with the diffusion constant D_ϕ. The omnipresent $1/f$ noise of oscillator components also causes phase fluctuations. The corresponding variances, $\sigma^2_{\Delta\phi,B}(\tau)$ and $\sigma^2_{\Delta\phi,1/f}(\tau)$, are given in [125, 126]. By using Eq. (17) the variance of the phase increments due to AD noise, $\sigma^2_{\Delta\phi,AD}(\tau)$, can be obtained, applying $S_{\Delta f}(\nu)=(f_0/2m)^2 S_{\Delta m}(\nu)$, where $S_{\Delta m}(\nu)$ is given by Eq. (12). We determined the variance $\sigma^2_{\Delta\phi,AD}(\tau)$ for single gas single-layer adsorption (by using Eqs. (13) and (17)) [122]. In the presence of these noises the corresponding variances are

$$\sigma^2_{\Delta\varphi,B}(\tau) = 2D_\varphi \tau\,,\ \sigma^2_{\Delta\varphi,1/f}(\tau) = K\tau^2\,,\ \sigma^2_{\Delta\varphi,AD}(\tau) = P[\tau - \tau_1(1-e^{-\tau/\tau_1})]/2 \tag{18}$$

where K is related to parameters of the $1/f$ noise in an oscillator circuit, and $P=g_{1e}(N_{1E})\tau_1^2 M_1^2 (f_0/2m)^2$. Assuming that mentioned noise sources are not correlated, the total variance equals the sum of the components that correspond to each of the frequency noise sources. The corresponding total autocorrelation function equals the product of the autocorrelation functions of all noise contributors. The individual spectra are denoted with $S_{\theta,B}(\nu)$, $S_{\theta,1/f}(\nu)$ and $S_{\theta,AD}(\nu)$, and they are obtained using Eqs. (16) and (18). The

PSD of $\theta(t)$, i.e. $S_\theta(\nu)$, is the convolution of the individual power spectra in the frequency domain. The oscillator phase noise, which includes the influence of the resonator AD noise, is then obtained from Eq. (15). The component which represents the contribution of the Lorentzian AD frequency noise of the resonator to the oscillator's total phase noise is [122]

$$S_{\theta,AD}(\nu) = 2\tau_1 \operatorname{Re}\left\{\frac{e^a}{a^z}\int_0^a t^{z-1}e^{-t}dt\right\} = 2\tau_1 \operatorname{Re}\left\{\frac{e^a}{a^z}\gamma(z,a)\right\} \tag{19}$$

where $\gamma(z,a)$ is the lower incomplete gamma function, $a=P\tau_1/4$, and $z=P\tau_1/4+j\omega\tau$, $\omega=2\pi\nu$.

3.3. Results of numerical calculations and discussion

By applying the derived theoretic model, we analyzed single layer adsorption on the surface of MEMS/NEMS silicon resonator with the nominal resonance frequency of 50 MHz (m=8.18·10^{-16} kg, A=8.89·10^{-12} m^2). Fig. 7a shows the dependence of the resonator AD phase noise ($L_R(\nu)=10\log(0.5(f_0/2m)^2S_{\Delta m}(\nu)/\nu^2)$ [123]) on the pressure of the gas inside the resonator's housing, at various offset frequencies from the nominal, at T=300 K, for the case of the resonator operating in a single gas atmosphere. The gas is nitrogen [123]. It can be observed that this noise has a low magnitude at near-atmospheric pressures, but becomes significant as the pressure decreases. This observation is very significant when optimization of operating conditions of MEMS/NEMS resonators is performed. In a majority of studies resonator TM noise is analyzed and the operating conditions are chosen so to minimize it. This means that low pressure values are chosen at which energy dissipation due to the surrounding medium is low enough, so TM is also reduced. At typical pressure values in evacuated MEMS/NEMS resonator packages, AD noise has its maximum, and, therefore, it can become dominant [115, 123]. Therefore, the optimization of operating conditions of RF MEMS/NEMS resonators in order to minimize their total noise must be performed based on the analysis of all the noises dependent on the ambient pressure and temperature. AD noise becomes increasingly important in such analysis with the increase of resonance frequencies, i.e. with the decrease of resonator dimensions, as can be seen in Fig. 7b.

AD phase noise of the same resonator, but operating in a two-gas atmosphere, is shown in Fig. 7c, as a function of both the gas 1 pressure (the gas 2 pressure is p_2=10^3 Pa, T=300 K) and the offset frequency. It can be observed that the presence of multiple gases affects resonator AD noise. In [116, 117] it is shown that in a certain pressure and frequency range the magnitude of the AD noise spectrum for two-gas adsorption is lower than for the case of one gas. However, since the decrease does not exist at all frequencies, the effect of the gas mixture composition on the total AD noise in the bandwidth of interest should be observed. The presented theory enables performing the analysis that yields the optimal gas mixture composition at which the resonator AD noise is minimized.

The PSD $S_{\theta,AD}(\nu)$ for a single gas atmosphere at different gas pressures [122] is shown in Fig. 7d, for the same example as shown in Fig. 7a. The pressure values are chosen: one of them approximates the pressure at which AD noise has its maximum, another one is an order of magnitude lower, and the remaining one an order of magnitude higher. This is the first result that illustrates the spectral dependence of the component of the oscillator phase

noise that is caused by the AD frequency noise. Its influence on oscillator noise must be analyzed together with the other two components ($S_{\theta,B}(\nu)$ and $S_{\theta,1/f}(\nu)$), by determining the total PSD of $\theta(t)$, i.e. $S_\theta(\nu)$ (as the convolution in the frequency domain of the three PSDs), and subsequently (based on Eq. (15)) obtaining the oscillator phase noise, which includes the influence of the resonator AD noise.

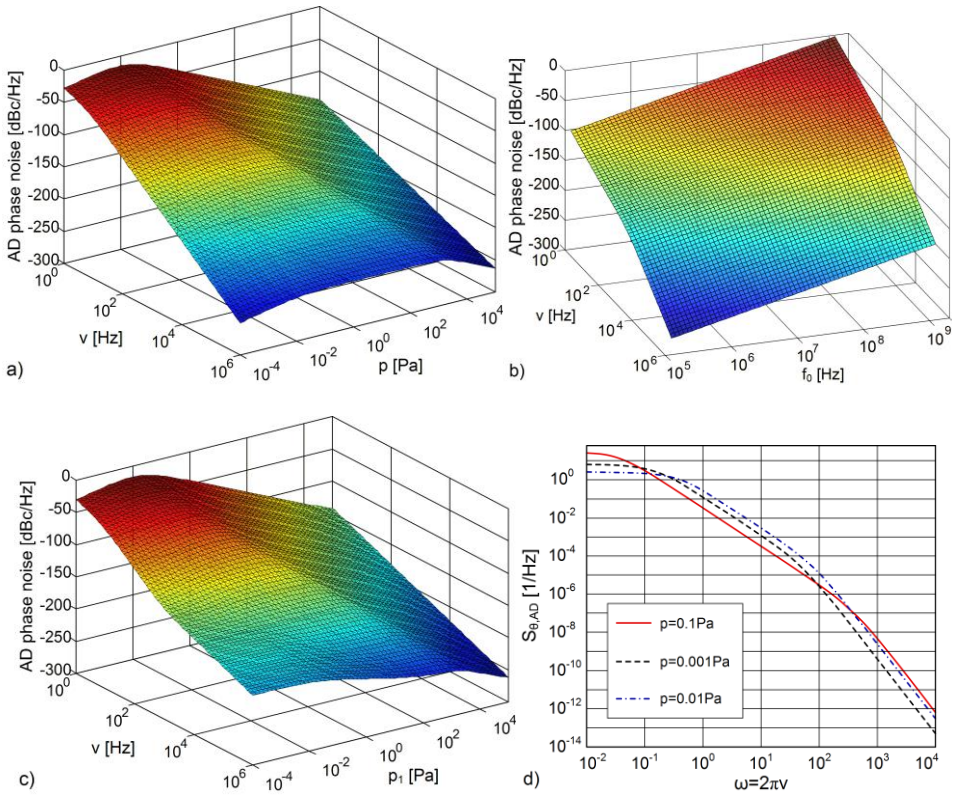

Fig. 7 a) Dependence of the MEMS/NEMS resonator AD phase noise (single gas single layer adsorption) on gas pressure and offset frequency (T=300 K, nitrogen, f_0=50 MHz), b) AD phase noise (single gas single layer adsorption) as a function of the resonance frequency (p=0.01 Pa), c) AD phase noise for a two-gas atmosphere, as a function of the gas 1 pressure and offset frequency (pressure of the gas 2 is $p_2=10^3$ Pa), d) The calculated PSD (Eq. (19)) of the oscillator phase noise constituent caused by AD process of a single gas of pressure p.

4. CONCLUSION

RF components based on MEMS and NEMS structures are expected to have an important role in achieving new levels of integration and reconfigurability of transceivers in future mobile terminals. MEMS/NEMS resonators have generated a significant interest

because of their ultra-high resonance frequencies, small size, very low operating power, high quality factors and possibility of integration with silicon IC technologies.

RF MEMS resonators have already become a competitive alternative to conventional components used for realization of RF filtering and frequency synthesis in wireless transceivers. Significant results achieved after the year 2000 (especially in terms of better temperature stability, better long-term stability, improved packaging) have enabled the commercialization of both piezoelectric and capacitive MEMS resonators.

Due to unique mechanical properties (enabling high resonance frequencies), especially their mechanical compliance needed for high frequency tunability, NEMS resonators, including 2D (graphene) resonators, provide a promising basis for future ultrafast communication systems. The studies in the field of NEMS are at the forefront of physical and engineering sciences. However, a number of issues need to be addressed in order to enable practical applications. There are problems that remain to be solved on both theoretic and experimental level. Most developments in this field are currently confined to theoretic models, simulations and laboratory experiments, with NEMS components in a prototype stage, at best.

Noise generation mechanisms in MEMS and NEMS resonant structures require further investigation in order for their ultimate performances to be determined. The extremely low mass and their large surface-to-volume ratio make these resonators highly sensitive to added mass. Therefore, stochastic adsorbed mass fluctuations influence the fluctuations of MEMS/NEMS resonator parameters, i.e. they are a source of adsorption-desorption (AD) noise which contributes to the resonator total noise. By analyzing the AD noise that becomes prominent as the dimensions and mass of the components decrease, we contributed to the theory of noise in MEMS and NEMS resonators, and subsequently to the theory of phase noise in oscillators using RF MEMS/NEMS resonators as frequency determining elements. The theoretical model of AD phase noise enables prediction of AD noise during the design of such components in order to identify the dominant noise generating mechanism, and then optimization of the resonator parameters and operating conditions in terms of noise minimization.

Acknowledgement. *This work was funded by the Serbian Ministry of Education, Science and Technological Development (Project TR 32008) and by the Serbian Academy of Sciences and Arts (Project F/150). The authors would like to express their gratitude to Prof. Dr. Gradimir Milovanović, full member of the Serbian Academy of Sciences and Arts, for his contribution in solving mathematical problems.*

REFERENCES

[1] J. Basu and T. K. Bhattacharyya, "Microelectromechanical Resonators for Radio Frequency Communication Applications", *Microsystem Technologies*, vol. 17, pp. 1557-1580, 2011.

[2] B. Kim, M. A. Hopcroft and R. N. Candler, "Silicon MEMS Resonators for Timing Applications", In *Microelectronics to Nanoelectronics Materials, Devices & Manu-facturability*, A. B. Kaul, Ed., CRC Press, 2012, pp. 79-108.

[3] J. T. M. van Beek and R. Puers, "A Review of MEMS Oscillators for Frequency Reference and Timing Applications", *J. Micromech. Microeng.*, vol. 22, pp. 013001 1-35, 2012.

[4] C. T.-C. Nguyen, "Vibrating RF MEMS Overview: Applications to Wireless Communications", In Proceedings of SPIE: Micromachining and Microfabrication Process Technology, vol. 5715, Photonics West: MOEMS-MEMS 2005, San Jose, California, 2005, pp. 11-25.

[5] D. E. Serrano, R. Tabrizian and F. Ayazi, "Tunable Piezoelectric MEMS Resonators for Real-Time Clock", In Proceedings of the Joint Conference of the IEEE International Frequency Control and the European Frequency and Time Forum (FCS), San Fransisco, CA, 2011, pp. 1-4.

[6] I. Voiculescu and A. N. Nordin, "Acoustic Wave Based MEMS Devices, Development and Applications", In: *Microelectromechanical Systems and Devices*, N. Islam, Ed., InTech, 2012, Chapter 4, pp. 65-86.

[7] R. Tabrizian, M. Rais-Zadeh and F. Ayazi, "Effect of Phonon Interactions on Limiting the f·Q Product of Micromechanical Resonators", In Proceedings of the International Solid-State Sensors, Actuators and Microsystems Conference (Transducers 2009), Denver, CO, 2009, pp. 2131–2134.

[8] C. Zuo, J. van der Spiegel and G. Piazza, "1.05-GHz CMOS Oscillator Based on Lateral Field-Excited Piezoelectric AlN Contour Mode MEMS Resonators", *IEEE Trans. Ultrason. Ferroelectr. Freq. Control*, vol. 57, pp. 82-87, 2010.

[9] G. Piazza, P. J. Stephanou, J. M. Porter, M. B. J. Wijesundara and A. P. Pisano, "Low Motional Resistance Ring-Shaped Contour-Mode Aluminium Nitride Piezoelectric Micromechanical Resonators for UHF Applications", In Proceedings of the 18th IEEE International Conference on Micro Electromechanical Systems (MEMS 2005), 2005, pp. 20-23.

[10] M. Rinaldi, C. Zuniga and G. Piazza, "5-10 GHz AlN Contour-Mode NanoElectroMechanical Resonators", In Proceedings of the 22nd IEEE International Conference on Micro Electro Mechanical Systems (MEMS 2009), 2009, pp. 916-919.

[11] H. M. Lavasani, P. Wanling, B. Harrington, R. Abdolvand and F. Ayazi, "A 76 dB 1.7 GHz 0.18 μm CMOS Tunable TIA using Broadband Current Pre-Amplifier for High Frequency Lateral Micromechanical Oscillators", *IEEE Journal of Solid-State Circuits*, vol. 46, pp. 224-235, Jan 2011.

[12] W.-C. Chen, W. Fang and S.-S. Li, "Quasi-Linear Frequency Tuning for CMOS-MEMS Resonators", In Proceedings of the 24th IEEE International Conference on Micro Electro Mechanical Systems (MEMS 2011), 2011, pp. 784-787.

[13] G. K. Ho, K. Sundaresan, S. Pourkamali and F. Ayazi, "Low-Motional-Impedance Highly-Tunable I^2 Resonators for Temperature Compensated Reference Oscillators", In Proceedings of the IEEE Micro Electro Mechanical Systems Conference (MEMS'05), Miami, FL, 2005, pp. 116-120.

[14] H. G. Barrow, T. L. Naing, R. A. Schneider, T. O. Rocheleau, V. Yeh, Z. Ren and C. T.-C. Nguyen, "A Real-Time 32.768-kHz Clock Oscillator Using a 0.0154-mm^2 Micromechanical Resonator Frequency-Setting Element", In Proceedings of the IEEE International Freq. Control Symposium, Baltimore, MD, 2012, pp. 1-6.

[15] Z. Hao, S. Pourkamali and F. Ayazi, "VHF Single-Crystal Silicon Elliptic Bulk-Mode Capacitive Disk Resonators–Part I: Design and Modeling", *J. Microelectromech. Syst.*, vol. 13, pp. 1043–1053, 2004.

[16] J. E. Y. Lee and A. A. Seshia, "5.4-MHz Single-Crystal Silicon Wine Glass Mode Disk Resonator with Quality Factor of 2 Million", *Sens. Actuators A*, vol. 156, pp. 28–35, 2009.

[17] J. Wang, J. E. Butler, T. Feygelson and C. T.-C. Nguyen, "1.51-GHz Polydiamond Micromechanical Disk Resonator with Impedance-Mismatched Isolating Support", In Proceedings of the 17th IEEE International Conference on Micro Electro Mechanical Systems, Maastricht, The Netherlands, 2004, pp. 641-644.

[18] Frederic Nabki, "Silicon Carbide Micro-Electromechanical Resonators for Highly Integrated Frequency Synthesizers", PhD thesis, McGill University, Montreal, Canada, 2009.

[19] K. Wang, A.-C. Wong and C. T.-C. Nguyen, "VHF Free–Free Beam High-Q Micromechanical Resonators", *IEEE/ASME J. Microelectromech. Syst.*, vol. 9, pp. 347-360, 2000.

[20] S. Pourkamali and F. Ayazi, "SOI-Based HF and VHF Single-Crystal Silicon Resonators with Sub-100 Nanometer Vertical Capacitive Gaps", In Proceedings of the 12th International Conference on Solid State Sensors, Actuators and Microsystems (Transducers '03), Boston, 2003, pp. 837-840.

[21] Y. Naito, P. Helin, K. Nakamura, J. De Coster, B. Guo, L. Haspeslagh, K. Onishi and H. Tilmans, "High-Q Torsional Mode Si Triangular Beam Resonators Encapsulated using SiGe Thin Film", In Proceedings of the IEEE International Electron Devices Meeting, San Francisco, 2010, pp. 154–157.

[22] T. J. Cheng and S. A. Bhave. "High-Q, Low Impendance Polysilicon Resonators with 10 nm Air Gaps", In Proceedings of the 23rd IEEE International Conference on Micro Electro Mechanical Systems (MEMS 2010), Wanchai, Hong Kong, 2010, pp. 695-698.

[23] V. Kaajakari, T. Mattila, A. Oja, J. Kiihamäki and H. Seppä, "Square-Extensional Mode Single-Crystal Silicon Micromechanical Resonator for Low-Phase-Noise Oscillator Applications", *IEEE Electron Device Lett.*, vol. 25, pp. 173–175, 2004.

[24] G. Wu, D. Xu, B. Xiong and Y. Wang, "A High-Performance Bulk Mode Single Crystal Silicon Micro-Resonator Based on a Cavity-SOI Wafer, *J. Micromech. Microeng*., vol. 22, pp. 025020 1-8, 2012.

[25] Y.-W. Lin, S.-S. Li, Z. Ren and C. T.-C. Nguyen, "Low Phase Noise Array-Composite Micromechanical Wine-Glass Disk Oscillator", In Proceedings of the IEEE International Electron Devices Meeting, Washington DC, 2005, pp. 287-290.

[26] M. U. Demirci, M. A. Abdelmoneum and C. T.-C. Nguyen, "Mechanically Corner-Coupled Square Microresonator Array for Reduced Series Motional Resistance", In Proceedings of the 12th International Conference on Solid-State Sensors & Actuators (Transducers'03), Boston, Massachussets, 2003, pp. 955-958.

[27] S.-S. Li, Y.-W. Lin, Y. Xie, Z. Ren and C. T.-C. Nguyen, "Micromechanical "Hollow-Disk" Resonators", In Proceedings of the 17th IEEE International Conference on.Micro Electro Mechanical Systems (MEMS 2004), 2004, pp. 821-824.

[28] P. Ovartchaiyapong, L. M. A. Pascal, B. A. Myers, P. Lauria and A. C. Bleszynski Jayich, "High Quality Factor Single-Crystal Diamond Mechanical Resonators", *Appl. Phys. Lett.*, vol. 101, pp. 163505 1-4, 2012.

[29] J. E.-Y. Lee and A. A. Seshia, "Square Wine Glass Mode Resonator with Quality Factor of 4 Million", In Proceedings of the 7th IEEE Conference on Sensors, Lecce, Italy, pp. 1257–1260, 2008.

[30] D. Weinstein and S. A. Bhave, "Internal Dielectric Transduction in Bulk-Mode Resonators", *J. Microelectromech. Syst.*, vol. 18, pp. 1401–1408, 2009.

[31] R. Henry and D. Kenny, "Comparative Analysis of MEMS, Programmable, and Synthesized Frequency Control Devices Versus Traditional Quartz Based Devices", In Proceedings of the IEEE Frequency Control Symposium, Honolulu, HI, 2008, pp. 396–401.

[32] J. L. Lopez, J. Verd, J. Teva, G. Murillo, J. Giner, F. Torres, A. Uranga, G. Abadal and N. Barniol, "Integration of RF-MEMS Resonators on Submicrometric Commercial CMOS Technologies", *J. Micromech. Microeng.*, vol. 19, pp. 015002 1-10, 2009.

[33] A. N. Nordin and M. E. Zaghloul, "Modeling and Fabrication of CMOS Surface Acoustic Wave Resonators", *IEEE Trans. on Microwave Theory Tech.*, vol. 55, pp. 992-1001, 2007.

[34] H. Campanella, E. Cabruja, E., J. Montserrat, A. Uranga, N. Barniol and J. Esteve, "Thin-Film Bulk Acoustic Wave Resonator Floating Above CMOS Substrate", *IEEE Electron Device Lett.*, vol. 29, pp. 28-30, 2008.

[35] M. Hara, J. Kuypers, T. Abe and M. Esashi, "MEMS Based Thin Film 2 GHz Resonator for CMOS Integration", In Proceedings of IEEE MTT-S International Microwave Symposium Digest, Philadelphia, PA, 2003, vol. 3, pp. 1797-1800.

[36] B. P. Otis and J. M. Rabaey, "A 300-μW 1.9-GHz CMOS Oscillator Utilizing Micromachined Resonators", *IEEE J. Solid-State Circuits*, vol. 38, pp. 1271-1274, 2003.

[37] J. S. Wang and K. M. Lakin, "Sputtered AlN Films for Bulk-Acoustic-Wave Devices", In Proceedings of Ultrasonics Symposium, Chicago, IL, 1981, pp. 502-505.

[38] M. A. Dubois, J. F. Carpentier P. Vincent, C. Billard, G. Parat, C. Muller, P. Ancey and P. Conti, "Monolithic Above-IC Resonator Technology for Integrated Architectures in Mobile and Wireless Communication", *IEEE J. Solid-State Circuits*, vol. 41, pp. 7–16, 2006.

[39] B. P. Harrington, M. Shahmohammadi and R. Abdolvand, "Toward Ultimate Performance in GHZ MEMS Resonators: Low Impedance and High Q", In Proceedings of the 23rd IEEE International Conference on Micro Electro Mechanical Systems (MEMS), Wanchai, Hong Kong, 2010, pp. 707-710.

[40] L. Khine, "Performance Parameters of Micromechanical Resonators", PhD. Thesis, National University of Singapore, 2010.

[41] J. Wang, Z. Ren and C. T.-C. Nguyen, "1.156-GHz Self-Aligned Vibrating Micromechanical Disk Resonator", *IEEE Trans. Ultrason. Ferroelect. Freq. Control*, vol. 51, pp. 1607-1628, 2004.

[42] K. Sundaresan, G. K. Ho, S. Pourkamali and F. Ayazi, "Electronically Temperature Compensated Silicon Bulk Acoustic Resonator Reference Oscillators", *IEEE J. Solid-State Circuits*, vol. 42, pp. 1425–1434, 2007.

[43] J. Salvia, M. Messana, M. Ohline, M. A. Hopcroft, R. Melamud, S. Chandorkar, H. K. Lee, G. Bahl, B. Murmann and T. W. Kenny, "Exploring the Limits and Practicality of Q-based Temperature Compensation for Silicon Resonators", In Proceedings of International Electron Devices Meeting, San Francisco, CA, 2008, pp. 1-4.

[44] W.-T. Hsu and C. T.-C. Nguyen, "Stiffness-Compensated Temperature Insensitive Micro-mechanical Resonators", In Proceedings of IEEE International Micro Electro Mechanical Systems Conference, Las Vegas, Nevada, 2002, pp. 731–734.

[45] A. K. Samarao and F. Ayazi, "Temperature Compensation of Silicon Micromechanical Resonators via Degenerate Doping", In Proceedings of IEEE International Electron Devices Meeting. Baltimore, 2009, pp. 1–4.

[46] A. K. Samarao, G. Casinovi and F. Ayazi, "Passive TCF Compensation in High Q Silicon Micromechanical Resonators", In Proceedings of the 23nd IEEE International Conference on Microelectromechanical Systems, Hong Kong, 2010, pp. 116–119.

[47] R. Melamud, S. A. Chandorkar, K. Bongsang, H. K. Lee, J. C. Salvia, G. Bahl, M. A. Hopcroft and T. W. Kenny, "Temperature Insensitive Composite Micromechanical Resonators", *J. Micro-electromechanical Systems*, vol. 18, pp. 1409–1419, 2009.

[48] H. K. Lee, M. A. Hopcroft, R. K. Melamud, B. Kim, J. Salvia, S. Chandorkar,ž and T. W. Kenny, "Electrostatic Tuning of Hermetically Encapsulated Composite Resonators", In Proceedings of IEEE Solid State Sensor, Actuator and Microsystems Workshop, Hilton Head, 2008, pp. 48–51.

[49] J. H. Seo, K. S. Demirci, A. Byun, S. Truax and O. Brand, "Novel Temperature Compensation Scheme for Microresonators Based on Controlled Stiffness Modulation", In Proceedings of International Conference on Solid-State Sensors, Actuators and Microsystems (Transducers 2007), 2007, pp. 2457–2360.

[50] H. Wan-Thai, J. R. Clark and C. Nguyen, "Mechanically Temperature-Compensated Flexural-Mode Micromechanical Resonators", In Proceedings of IEEE International Electron Devices Meeting, San Francisco, CA, 2000, pp. 399-402.

[51] F. Nabki, T. A. Dusatko and M. N. El-Gamal, "Frequency Tunable Silicon Carbide Resonators for MEMS Above IC", In Proceedings of IEEE Custom Integrated Circuits Conference, San Jose, CA, 2008, pp. 185-188.

[52] W. Pang, H. Zhang, H. Yu, C.-Y. Lee and E. S. Kim, "Electrical Frequency Tuning of Film Bulk Acoustic Resonator", *J. Microelectromechanical Systems*, vol. 16, pp. 1303-1313, 2007.

[53] M. Lutz, A. Partridge and P. Gupta, N. Buchan, E. Klaassen, J. McDonald and K. Petersen, "MEMS Oscillators for High Volume Commercial Applications", In Proceedings of the 14th IEEE International Conference on Solid State Sensors, Actuators and Microsystems, 2007, pp. 49–52.

[54] W. T. Hsu, "Reliability of Silicon Resonator Oscillators", In Proceedings of IEEE International Frequency Control Symposium and Exposition, Miami, FL, 2006, pp. 389–392.

[55] M. Lutz, J. McDonald, P. Gupta, A. Partridge, C. Dimpel and K. Petersen, "New MEMS Timing References for Automotive Applications", In *Advanced Microsystems for Automotive Applications*, J. Valldorf, W. Gessner, Eds., Berlin: Springer, 2007, pp. 279-289.

[56] Y. W. Lin, S. Lee, Z. Ren and C. T.-C. Nguyen, "Series-Resonant Micromechanical Resonator Oscillator", In Proceedings of IEEE International Electron Devices Meeting, Washington, DC, 2003, pp. 39.4.1–39.4.4.

[57] T. Mattila, O. Jaakkola, J. Kiihamaki, J. Karttunen, T. Lamminmaki, P. Pantakari, A. Oja, H. Seppa, H. Kattelus and I. Tittonen, "14 MHz Micromechanical Oscillator", *Sens. Actuators A*, vol. 97-98, pp. 497-502, 2002.

[58] M. Sworowski, F. Neuilly, B. Legrand, A. Summanwar, P. Philippe and L. Buchaillot, "Fabrication of 24-MHz-Disk Resonators with Silicon Passive Integration Technology", *IEEE Electron Device Lett.*, vol. 31, pp. 23–25, 2010.

[59] H. Lavasani, A. K. Samarao, G. Casinovi and F. Ayazi, "A 145 MHz Low Phase-Noise Capacitive Silicon Micromechanical Oscillator", In Proceedings of International Electron Devices Meeting, San Francisco, CA, 2008, pp. 675–678.

[60] P. Rantakari, V. Kaajakari, T. Mattila, J. Kiihamoki, A. Oja, I. Tittonen and H. Seppa, "Low Noise, Low Power Micromechanical Oscillator", In Proceedings of the 13th International Conference on Solid-State Sensors, Actuators and Microsystems (Transducers), Seoul, 2005, vol. 2, pp. 2135–2138.

[61] M. Akgul, B. Kim, L. W. Hung, Y. Lin, W.-C. Li, W.-L. Huang, I. Gurin, A. Borna and C. T.-C. Nguyen, "Oscillator Far-From Carrier Phase Noise Reduction via Nano-Scale Gap Tuning of Micromechanical Resonators", In Proceedings of the Solid-State Sensors, Actuators and Microsystems Conference (Transducers), Denver, CO, 2009, pp. 798–801.

[62] M. Ziaei-Moayyed, J. Hsieh, J.-W. P. Chen, E. P. Quevy, D. Elata and R. T. Howe, "Higher-Order Mode Internal Electrostatic Transduction of a Bulk-Mode Ring Resonator on a Quartz Substrate", In

Proceedings of the 17th International Solid-State Sensors, Actuators and Microsystems Conference (Transducers), Denver, CO, 2009, pp. 2338–2341.

[63] V. Kaajakari, T. Mattila, J. Kiihamaki, H. Kattelus, A. Oja and H. Seppa, "Nonlinearities in Single-Crystal Silicon Micromechanical Resonators", In Proceedings of the 12th International Conference on Solid State Sensors, Actuators and Microsystems, Boston, MA, 2003, pp. 1574–1577.

[64] M. U. Demirci and C. Nguyen, "Mechanically Corner-Coupled Square Microresonator Array for Reduced Series Motional Resistance", *IEEE/ASME J. Microelectromechanical Systems*, vol. 15, pp. 1419-1436, Dec. 2006.

[65] C.T.-C. Nguyen, "MEMS Technology for Timing and Frequency Control", *IEEE Trans. Ultrason. Ferroelect. Freq. Control*, vol. 54, pp. 251-270, 2007.

[66] Y. T. Yang, K. L. Ekinci, X. M. H. Huang, L. M. Schiavone, M. L. Roukes, C. A. Zorman and M. Mehregany, "Monocrystalline Silicon Carbide Nanoelectromechanical Systems", *Appl. Phys. Lett.*, vol. 78, pp. 162-164, 2001.

[67] H. A. C. Tilmans, M. Elwenspoek and J. H. J. Fluitman, "Micro Resonant Force Gauges", *Sens. Actuators A*, vol. 30, pp. 35-53, 1992.

[68] C. Chen, S. Lee, V. V. Deshpande, G.-H. Lee, M. Lekas, K. Shepard and J. Hone, "Graphene Mechanical Oscillators with Tunable Frequency", *Nat. Nanotechnol.*, vol. 8, pp. 923-927, 2013.

[69] A. N. Cleland and M. L. Roukes, "Fabrication of High Frequency Nanometer Scale Mechanical Resonators from Bulk Si Crystals", *Appl. Phys. Lett.*, vol. 69, pp. 2653-2655, 1996.

[70] K. L. Ekinci and M. L. Roukes, "Nanoelectromechanical systems", *Rev. Sci. Instrum.*, vol. 76, pp. 061101, 2005.

[71] X. L. Feng, R. R. He, P. D. Yang and M. L. Roukes, "Very High Frequency Silicon Nanowire Electromechanical Resonators", *Nano Lett.*, vol. 7, pp. 1953-1959, 2007.

[72] X. M. H. Huang, X. L. Feng, C. A. Zorman, M. Mehregany and M. L. Roukes, "VHF, UHF and Microwave Frequency Nanomechanical Resonator", *New J. Phys.*, vol. 7, pp. 247 1-15, 2005.

[73] D. W. Carr, S. Evoy, L. Sekaric, H. G. Craighead and J. M. Parpia, "Measurements of Mechanical Resonance and Losses in Nanometer Scale Silicon Wires", *Appl. Phys. Lett.*, vol. 75, pp. 920-922, 1999.

[74] X. M. H. Huang, C. A. Zorman, M. Mehregany and M. L. Roukes, "Nanodevice Motion at Microwave Frequencies", *Nature*, vol. 421, pp. 496-496, 2003.

[75] A. N. Cleland, M. Pophristic and I. Ferguson, "Single-Crystal Aluminum Nitride Nanomechanical Resonators", *Appl. Phys. Lett.*, vol. 79, pp. 2070-2072, 2001.

[76] L. Sekaric, J. M. Parpia, H. G. Craighead, T. Feygelson, B. H. Houston and J. E. Butler, "Nanomechanical Resonant Structures in Nanocrystalline Diamond", *Appl. Phys. Lett.*, vol. 81, pp. 4455-4457, 2002.

[77] R. B. Karabalin, M. H. Matheny, X. L. Feng, E. Defaÿ, G. Le Rhun, C. Marcoux, S. Hentz, P. Andreucci and M. L. Roukes, "Piezoelectric Nanoelectromechanical Resonators Based on Aluminum Nitride Thin Films", *Appl. Phys. Lett.*, vol. 95, pp. 103111 1-3, 2009.

[78] A. Husain, J. Hone, H. W. Ch. Postma, X. M. H. Huang, T. Drake, M. Barbic, A. Scherer and M. L. Roukes,"Nanowire-Based Very-High-Frequency Electromechanical Resonator", *Appl. Phys. Lett.*, vol. 83, pp. 1240-1242, 2003.

[79] T. F. Li, Y. Pashkin, O. Astafiev, Y. Nakamura, J. S. Tsai and H. Im, "High-Frequency Metallic Nanomechanical Resonators", *Appl. Phys. Lett.*, vol. 92, pp. 043112 1-3, 2008.

[80] N. A. Melosh, A. Boukai, F. Diana, B. Gerardo, A. Badolato, P. M. Petroff and J. R. Heath, "Ultrahigh-Density Nanowire Lattices and Circuits", *Science*, vol. 300, pp. 112-115, 2003.

[81] X. L. Feng, M. H. Matheny, C. A. Zorman, M. Mehregany and M. L. Roukes, "Low Voltage Nanoelectromechanical Switches Based on Silicon Carbide Nanowires", *Nano Lett.*, vol. 10, pp. 2891-2896, 2010.

[82] O. Vazquez-Mena, G. Villanueva, V. Savu, K. Sidler, M. A. F. van den Boogaart and J. Brugger, "Metallic Nanowires by Full Wafer Stencil Lithography", *Nano Lett.*, vol. 8, pp. 3675-3682, 2008.

[83] R. He, D. Gao, R. Fan, A. I. Hochbaum, C. Carraro, R. Maboudian and P. Yang, "Si Nanowire Bridges in Microtrenches: Integration of Growth into Device Fabrication", *Adv. Mater.*, vol. 17, pp. 2098-2102, 2005.

[84] R. R. He, X. L. Feng, M. L. Roukes and P. D. Yang, "Self-Transducing Silicon Nanowire Electromechanical Systems at Room Temperature", *Nano Lett.*, vol. 8, pp. 1756-1761, 2008.

[85] C. Regal, J. Teufel and K. Lehnert, "Measuring Nanomechanical Motion with a Microwave Cavity Interferometer", *Nat. Physics*, vol. 4, pp. 555–560, 2008.

[86] S. T. Bartsch, A. Lovera, D. Grogg and A. M. Ionescu, "Nanomechanical Silicon Resonators with Intrinsic Tunable Gain and Sub-nW Power Consumption", *ACS Nano*, vol. 6, pp. 256–264, 2012.
[87] B. M. Zwickl, W. E. Shanks, A. M. Jayich, C. Yang, A. C. Bleszynski Jayich, J. D. Thompson and J. G. E. Harris, "High Quality Mechanical and Optical Properties of Commercial Silicon Nitride Membranes, *Appl. Phys. Lett.*, vol. 92, pp. 103125 1-3, 2008.
[88] S. Iijima, "Helical Microtubules of Graphitic Carbon", *Nature*, vol. 354, pp. 56-58, 1991.
[89] S. M. Huang, X. Y. Cai and J. Liu, "Growth of Millimeter-Long and Horizontally Aligned Single-Walled Carbon Nanotubes on Flat Substrates", *J. Amer. Chem. Soc.*, vol. 125, pp. 5636-5637, 2003.
[90] H. W. Zhu, C. L. Xu, D. H. Wu, B. Q. Wei, R. Vajtai and P. M. Ajayan, "Direct Synthesis of Long Single-Walled Carbon Nanotube Strands", *Science*, vol. 296, pp. 884-886, 2002.
[91] P. Poncharal, Z. L. Wang, D. Ugarte and W. A. de Heer, "Electrostatic Deflections and Electromechanical Resonances of Carbon Nanotubes", *Science*, vol. 283, pp. 1513-1516, 1999.
[92] V. Sazonova, Y. Yaish, H. Üstünel, D. Roundy, T. A. Arias and P. L. McEuen, "A Tunable Carbon Nanotube Electromechanical Oscillator", *Nature*, vol. 431, pp. 284-287, 2004.
[93] Vera Sazonova, "A Tunable Carbon Nanotube Resonator", PhD. Thesis, Cornell University, 2006.
[94] H. B. Peng, C. W. Chang, S. Aloni, T. D. Yuzvinsky and A. Zettl, "Ultrahigh Frequency Nanotube Resonators", *Phys. Rev. Lett.*, vol. 97, pp. 087203 1-4, 2006.
[95] D. Garcia-Sanchez, A. San Paulo, M. J. Esplandiu, F. Perez-Murano, L. Forró, A. Aguasca and A. Bachtold, "Mechanical Detection of Carbon Nanotube Resonator Vibrations", *Phys. Rev. Lett.*, vol. 99, pp. 085501 1-4, 2007.
[96] E. A. Laird, F. Pei, W. Tang, G. A. Steele and L. P. Kouwenhoven, "A High Quality Factor Carbon Nanotube Mechanical Resonator at 39 GHz", *Nano Lett.*, vol. 12, pp. 193–197, 2011.
[97] Chung-Chiang Wu, "Carbon Based Nanoelectromechanical Resonators", PhD. Thesis, University of Michigan, 2012.
[98] M. Imboden and P. Mohanty, "Dissipation in Nanoelectromechanical Systems", *Physics Reports*, vol. 534, pp. 89–146, 2014.
[99] B. Lassagne, D. Garcia-Sanchez, A. Aguasca and A. Bachtold, "Ultrasensitive Mass Sensing with a Nanotube Electromechanical Resonator", *Nano Lett.*, vol. 8, pp. 3735–3738, 2008.
[100] A. Huttel, G. Steele, B. Witkamp, M. Poot, L. Kouwenhoven and H. van der Zant, "Carbon Nanotubes as Ultrahigh Quality Factor Mechanical Resonators", *Nano Lett.*, vol. 9, pp. 2547–2552, 2009.
[101] Benjamin Jose Aleman, "Carbon Nanotube and Graphene Nanoelectromechanical Systems", PhD. Thesis, University of California, Berkeley, 2011.
[102] A. K. Geim, K. S. Novoselov, "The Rise of Graphene", *Nat. Mater.*, vol. 6, pp. 183–191, 2007.
[103] J. S. Bunch, A. M. van der Zande, S. S. Verbridge, I. W. Frank, D. M. Tanenbaum, J. M. Parpia, H. G. Craighead and P. L. McEuen, "Electromechanical Resonators from Graphene Sheets", *Science*, vol. 315, pp. 490-493, 2007.
[104] D. Garcia-Sanchez, A. M. van der Zande, A. San Paulo, B. Lassagne, P. L. McEuen A. Bachtold, "Imaging Mechanical Vibrations in Suspended Graphene Sheets", *Nano Lett.*, vol. 8, pp. 1399-1403, 2008.
[105] C. Y. Chen, S. Rosenblatt, K. I. Bolotin, W. Kalb, P. Kim, I. Kymissis, H. L. Stormer, T. F. Heinz and J. Hone, "Performance of Monolayer Graphene Nanomechanical Resonators with Electrical Readout", *Nat. Nanotech.*, vol. 4, pp. 861-867, 2009.
[106] R. A. Barton, B. Ilic, A. M. van der Zande, W. S. Whitney, P. L. McEuen, J. M. Parpia and H. G. Craighead, "High, Size-Dependent Quality Factor in an Array of Graphene Mechanical Resonators", *Nano Lett.*, vol. 11, pp. 1232–1236, 2011.
[107] Y. S. Greenberg, Y. A. Pashkin and E. Il'ichev, "Nanomechanical Resonators", *Physics – Uspekhi*, vol. 55, pp. 382-407, 2012.
[108] Z. Djurić, "Mechanisms of Noise Sources in Microelectromechanical Systems", Introductory invited paper, *Microelectron. Reliab.*, vol. 40, pp. 919-932, 2000.
[109] F. L. Walls and J. R. Vig, "Fundamental Limits on the Frequency Stabilities of Crystal Oscillators", *IEEE Trans. Ultrason. Ferroel. Freq.Contro*l, vol. 42, pp. 576-589, 1995.
[110] J. R. Vig and Y. Kim, "Noise in MEMS Resonators", *IEEE Trans. Ultrason. Ferroelect. Freq. Control*, vol. 46, pp. 1558-1565, 1999.
[111] A. N. Cleland and M. L. Roukes, "Noise Processes in Nanomechanical Resonators", *J. Appl. Lett.*, vol. 92, pp. 2758-2769, 2002.

[112] Z. Djurić, "Noise in Nanoelectromechanical Systems", Invited paper, In Proceedings of the 1st International Workshop on Nanoscience & Nanotechnology IWON 2005, Belgrade, Serbia and Montenegro, 2005, pp. 33-36.

[113] Z. Djurić, "Noise in Microsystems and Semiconductor Photodetectors", In Proceedings of the XLIV Conference ETRAN, Sokobanja, Serbia, 2000, pp. 9-16.

[114] Y. K. Yong and J. R. Vig, "Resonator Surface Contamination – A Cause of Frequency Fluctuations?", *IEEE Trans. Ultrason. Ferroelect. Control*, vol. 36, pp. 452-458, 1989.

[115] Z. Djurić, O. Jakšić and D. Randjelović, "Adsorption–Desorption Noise in Micromechanical Resonant Structures", *Sens. Actuators* A, vol. 96, pp. 244-251, 2002.

[116] Z. Djurić, I. Jokić, M. Frantlović, O. Jakšić and D. Vasiljević-Radović, "Adsorbed Mass and Resonant Frequency Fluctuations of a Microcantilever Caused by Adsorption and Desorption of Particles of Two Gases", In Proceedings of the 24th International Conference on Microelectronics MIEL 2004, vol. 1, Niš, Serbia, 2004, pp. 197-200.

[117] Z. Djurić, I. Jokić, M. Frantlović and O. Jakšić, "Fluctuations of the Number of Particles and Mass Adsorbed on the Sensor Surface Surrounded by a Mixture of an Arbitrary Number of Gases", *Sens. Actuators B*, vol. 127, pp. 625-631, 2007.

[118] I. Jokić, Z. Djurić, M. Frantlović, K. Radulović, P. Krstajić and Z. Jokić, "Fluctuations of the Number of Adsorbed Molecules in Biosensors due to Stochastic Adsorption–Desorption Processes Coupled with Mass Transfer", *Sens. Actuators* B, vol. 166–167, pp. 535–543, 2012.

[119] M. Frantlović, I. Jokić, Z. Djurić and K. Radulović, "Analysis of the Competitive Adsorption and Mass Transfer Influence on Equilibrium Mass Fluctuations in Affinity-Based Biosensors", *Sens. actuators B*, vol. 189, pp. 71-79, 2013.

[120] Z. Djurić, I. Jokić, M. Frantlović and K. Radulović, "Two-Layer Adsorption and Adsorbed Mass Fluctuations on Micro/Nanostructures", *Microel. Eng.*, vol. 86, pp. 1278-1281, 2009.

[121] Z. Djurić, I. Jokić, M. Djukić and M. Frantlović, "Fluctuations of the Adsorbed Mass and the Resonant Frequency of Vibrating MEMS/NEMS Structures due to Multilayer Adsorption", *Microel. Eng.*, vol. 87, pp. 1181-1184, 2010.

[122] I. Jokić, M. Frantlović and Z. Djurić, "RF MEMS and NEMS Components and Adsorption-Desorption Induced Phase Noise", In Proceedings of the 29th International Conference on Microelectronics MIEL 2014, Belgrade, Serbia, 2014, pp. 117-124.

[123] I. Jokić, M. Frantlović, Z. Djurić and M. Dukić, "Adsorption-Desorption Phase Noise in RF MEMS/NEMS Resonators", In Proceedings of the 10th International Conference on Telecommunications in Modern Satellite, Cable and Broadcasting Services TELSIKS, Niš, Serbia, 2011, pp. 114-117.

[124] K.M. van Vliet and J.R. Fasset, "Fluctuations due to Electronic Transitions and Transport in Solids", in *Fluctuation Phenomena in Solids*, R. E. Burgess, Ed., New York and London: Academic Press, 1965, pp. 267-354.

[125] S. Yousefi, T. Eriksson and D. Kuylenstierna, "A Novel Model for Simulation of RF Oscillator Phase Noise", In Proceedings of the IEEE Radio and Wireless Symposium, New Orleans, 2010, pp.428-431.

[126] G. V. Klimovitch, "Near-Carrier Oscillator Spectrum due to Flicker and White Noise", In Proceedings of the IEEE International Symposium on Circuits and Systems ISCAS 2000, vol. 1, Geneva, 2000, pp.703-706.

[127] M. J. Buckingham, *Noise in Electronic Devices and Systems*, Ellis Horwood Ltd., 1983.